

SIMC 2.0: Improved Secure ML Inference Against Malicious Clients

Guowen Xu, Xingshuo Han, Tianwei Zhang, Hongwei Li, *Senior Member, IEEE*, Robert H.Deng *Fellow, IEEE*

Abstract— In this paper, we study the problem of secure ML inference against a malicious client and a semi-trusted server such that the client only learns the inference output while the server learns nothing. This problem is first formulated by Lehmkuhl *et al.* with a solution (MUSE, Usenix Security’21), whose performance is then substantially improved by Chandran *et al.*’s work (SIMC, USENIX Security’22). However, there still exists a nontrivial gap in these efforts towards practicality, giving the challenges of overhead reduction and secure inference acceleration in an all-round way.

We propose SIMC 2.0, which complies with the underlying structure of SIMC, but significantly optimizes both the linear and non-linear layers of the model. Specifically, (1) we design a new coding method for homomorphic parallel computation between matrices and vectors. It is custom-built through the insight into the complementarity between cryptographic primitives in SIMC. As a result, it can minimize the number of rotation operations incurred in the calculation process, which is very computationally expensive compared to other homomorphic operations (*e.g.*, addition, multiplication). (2) We reduce the size of the garbled circuit (GC) (used to calculate nonlinear activation functions, *e.g.*, ReLU) in SIMC by about two thirds. Then, we design an alternative lightweight protocol to perform tasks that are originally allocated to the expensive GCs. Compared with SIMC, our experiments show that SIMC 2.0 achieves a significant speedup by up to $17.4\times$ for linear layer computation, and at least $1.3\times$ reduction of both the computation and communication overheads in the implementation of non-linear layers under different data dimensions. Meanwhile, SIMC 2.0 demonstrates an encouraging runtime boost by $2.3 \sim 4.3\times$ over SIMC on different state-of-the-art ML models.

Index Terms—Privacy Protection, Secure Inference, Homomorphic Encryption, Garbled Circuit.

The widespread application of machine learning (ML), especially the popularization of prediction services over pre-trained models, has increased the demand for *secure inference*. In this process, a server S_0 holds an ML model M whose weight W is considered private and sensitive, while a client S_1 holds a private input t . The goal of secure inference is to make S_1 only get the model’s output while S_0 knows nothing. Such a privacy-preserving paradigm has a variety of potential prospects, especially for privacy-critical applications, *e.g.*, medical diagnosis, financial data analysis. In theory, secure inference can be implemented by the secure two-party computing (2-PC) protocol in cryptographic primitives [1], [2].

Guowen Xu, Xingshuo Han, and Tianwei Zhang are with the School of Computer Science and Engineering, Nanyang Technological University. (e-mail: guowen.xu@ntu.edu.sg; xingshuo001@e.ntu.edu.sg; tianwei.zhang@ntu.edu.sg)

Hongwei Li is with the School of Computer Science and Engineering, University of Electronic Science and Technology of China, Chengdu 611731, China.(e-mail: hongweili@uestc.edu.cn)

Robert H Deng is with the School of Information Systems Singapore Management University. (e-mail: robertdeng@smu.edu.sg)

It enables two parties to run an interactive protocol to securely calculate any function without revealing each party’s private information. To instantiate it, a lot of impressive works [3], [4], [5] have been proposed, and they are built on various cryptographic technologies such as homomorphic encryption (HE), secret sharing, and Yao’s garbled circuits (GC). Due to the inherent complexity of cryptographic primitives, existing efforts exclusively focus on improving the efficiency and lie on a relatively weak threat assumption, *i.e.*, the *semi-honest adversary model* [6], [7], [8]. In this model, S_0 and S_1 faithfully follow the specifications of secure inference and can only capture private information through passive observations.

A. Related Works

Recent works [9], [10], [11] show that this *semi-honest adversary model* can be insecure in real-world applications. Particularly, Lehmkuhl *et al.* [9] argue that it may be reasonable the ML model is held by a semi-trusted server, since the server is usually fixed and maintained by a reputable entity. However, it is impractical to assume that thousands of clients (which can be arbitrary entities) will faithfully comply with the protocol specification. To validate this hazard, they provide a systematic attack strategy, which enables a malicious client to violate the rules of the protocol and completely reconstruct the model’s parameters during the inference interactions. Moreover, the number of inference queries required for such an attack is far smaller than the most advanced black-box model extraction attack.

While the above problem can be solved by resorting to the traditional 2-PC protocol against malicious adversaries [12], [13], [14], it is inefficient in practice. To bridge this gap, Lehmkuhl *et al.* [9] pioneer the definition of *client-malicious adversary model*, where the server is still considered semi-honest but the client can perform arbitrary malicious behaviors. To secure the inference process under such adversary model, they propose MUSE, a novel 2-PC protocol with considerably lower overhead compared to previous works. However, the computation and communication costs of MUSE are still not satisfactory, which are at least $15\times$ larger than the similar work DELPHI [15] under the semi-trusted threat model.

To alleviate the efficiency issue, Chandran *et al.* design SIMC [10], the state-of-the-art 2-PC protocol for secure inference under the client-malicious adversary model. Consistent with the underlying tone of MUSE, SIMC uses HE to execute the linear layers (including matrix-vector and convolution multiplication) of the ML model, and uses GC to implement

the non-linear layers (mainly the ReLU function). Since almost 99% of the communication overhead in MUSE comes from non-linear layers, the core of SIMC is a novel protocol based on a customized GC to improve the performance of executing non-linear activation functions. As a result, compared with MUSE, SIMC gains $28 \sim 33\times$ reduction in the communication overhead for the implementation of popular activation functions (*e.g.*, ReLU, ReLU6), and at least $4\times$ overall performance improvement.

However, we argue that SIMC is still far from practicality. This stems from two reasons. First, SIMC keeps the design of linear layer calculations in MUSE, which uses computationally heavy HE to perform dense matrix-vector and convolution multiplication. Actually, linear operations dominate the computation of modern neural networks: nearly 95% of ML model execution is for intensive convolutional layers and fully connected (FC) layers [16]. This raises the requirement for efficient execution of matrix and convolution multiplication under ciphertext. Although the homomorphism of HE makes it suitable to achieve privacy-preserving linear operations, it is still computationally expensive for large-scale operations, especially when there is no appropriate parallel computing optimization (*i.e.*, performing homomorphic linear computation in a Single Instruction Multiple Data (SIMD) manner) [17].

There is still much optimization space for the non-linear layers (such as ReLU) of SIMC, from the perspectives of both computation and communication. To be precise, given secret shares of a value t , SIMC designs a GC-based secure 2-PC protocol, which enables S_0 and S_1 to calculate shares $s = \alpha t$ and authenticated shares of $v = f(t)$, *i.e.*, shares of $f(t)$ and $\alpha f(t)$, where f denotes the activation function. While SIMC has made great efforts to simplify the design of the GC and prevent malicious behaviors from the client, it requires the communication overhead of at least $2c\lambda + 4\kappa\lambda + 6\kappa^2$, where λ denotes the security parameter, κ is a field space, and c is the number of AND gates required to reconstruct shares of t and compute authenticated $f(t)$. Besides, the main body of the activation function is still sealed in a relatively complex GC. As a consequence, SIMC inevitably results in substantial computation and communication costs in non-linear layers, since a modern model usually contains thousands of non-linear activation functions for calculation. We will perform experiments to demonstrate such overheads in Section V.

B. Technical Challenges

This paper is dedicated to design a new 2-PC protocol to break through the performance bottleneck in SIMC, thereby promoting the practicality of secure inference against malicious clients. We follow the underlying structure of SIMC, *i.e.*, using HE to execute the linear layers and GC to implement the non-linear layers, as such a hybrid method has shown advanced performance compared to other strategies [9], [15]. Therefore, our work naturally lie in solving two problems: (1) how to design an optimized mechanism to accelerate linear operations in HE, and (2) how to find a more simplified GC for the execution of non-linear activation functions.

There have been many impressive works [18], [19], [17], [16] exploring methods towards the above goals. To speed up HE's computation performance, existing efforts mainly focus on designing new coding methods to achieve parallelized component-wise homomorphic computation, *i.e.*, performing homomorphic linear computation in an SIMD manner. For example, Jiang *et al.* [19] present a novel matrix encoding method for basic matrix operations, *e.g.*, multiplication and transposition. Compared with previous approaches, this method reduces the computation complexity of multiplying two $d \times d$ matrices from $O(d^3)$ to $O(d)$. However, it is exclusively applicable to matrix operations between square or rectangular matrices, but unfriendly to arbitrary matrix-vector multiplication and convolution operations in ML. In addition, it considers parallel homomorphic calculations in a full ciphertext environment, contrary to our scenario where only the input of the client is ciphertext while the model parameters are clear. Sav *et al.* [17] propose the Alternating Packing (AP) approach, which packs all plaintext elements of a vector into a ciphertext and then parallelizes the homomorphic matrix-vector multiplication. However, similar to [19], AP focuses on the SIMD operation between two packed ciphertexts.

Several works design solutions for the scenario of secure inference [20], [21], [16], mostly built on the *semi-honest adversary model*. Among them, one of the most remarkable works is GAZELLE [20]. It is customized for the HE-GC based secure inference, and has been integrated into some advanced solutions such as DELPHI [15] and EzPC [22]. In fact, the core idea of GAZELLE is also used in the design of MUSE and SIMC, which inherit DELPHI's optimization strategy for HE-based linear operations. GAZELLE builds a new homomorphic linear algebra kernel, which provides fast algorithms for mapping neural network layers to optimized homomorphic matrix-vector multiplication and convolution routines. However, the computation complexity of GAZELLE is still non-negligible. For example, to calculate the product of a $n_o \times n_i$ plaintext matrix and a n_i -dimensional ciphertext vector, GAZELLE requires at least $(\log_2(\frac{n}{n_o}) + \frac{n_i n_o}{n} - 1)$ rotation operations, where n is the number of slots in the ciphertext. This is very computationally expensive compared to other homomorphic operations such as addition and multiplication. To alleviate this problem, Zhang *et al.* [16] present GALA, an optimized solution over GAZELLE, to reduce the complexity of the rotation operations required by matrix vector calculations from $(\log_2(\frac{n}{n_o}) + \frac{n_i n_o}{n} - 1)$ to $(\frac{n_i n_o}{n} - 1)$, thus substantially improving the efficiency. However, GALA is specially customized for the secure inference under the *semi-honest adversary model*. In addition, we will demonstrate that the computation complexity of GALA is not optimal and can be further optimized.

To construct an efficient GC-based protocol, the following problems generally need to be solved: (1) avoiding using the GC to perform the multiplication between elements as much as possible, which usually requires at least $O(\kappa^2\lambda)$ communication complexity [23]; (2) ensuring the correctness of the client's input, so that the output of the GC is trusted and can be correctly propagated to the subsequent layers. SIMC presents a novel protocol that can meet these two requirements.

Specifically, instead of using the GC directly to calculate $s = \alpha t$ and authenticated shares of $v = f(t)$, SIMC only resorts to the GC to obtain the garbled labels of the bits corresponding to each function, namely $s[i], v[i]$ and $\alpha v[i]$ for $1 \leq i \leq \kappa$. Such types of calculation is natural for the GC because it operates on a Boolean circuit. Moreover, it avoids performing a large number of multiplication operations in the GC to achieve the binary-to-decimal conversion. Then, SIMC designs a lightweight input consistency verification method, which is used to force the client to feed the correct sharing of GC’s input. Compared with MUSE, SIMC reduces the communication overhead of each ReLU function from $2d\lambda + 190\kappa\lambda + 232\kappa^2$ to $2c\lambda + 4\kappa\lambda + 6\kappa^2$, and accelerates the calculation by several times.

We point out that it is possible to further simplify the protocol in SIMC. It stems from the insight that the ReLU function can be parsed as $f(t) = t \cdot \text{sign}(t)$, where the sign function $\text{sign}(t)$ equals 1 if $t \geq 0$ and 0 otherwise. Therefore, it is desirable if only the non-linear part of $f(t)$ (i.e., $\text{sign}(t)$) is encapsulated into the GC, i.e., for $1 \leq i \leq \kappa$, the output of the GC is $\text{sign}[i]$ and $s[i]$, instead of $s[i]$ and $v[i]$. Then, if we can find a lightweight alternative sub-protocol to privately compute the authenticated shares $v[i] = \text{sign}[i] \times s[i]$, it not only simplifies the size of the GC, but also further reduces the number of expensive multiplications between elements in the original GC. However, it is challenging to build such a protocol: the replacement sub-protocol should be lightweight compared to the original GC. In addition, it should be compatible with the input consistency verification method in SIMC, so as to realize the verifiability of the clients input.

C. Our Contributions

In this work, we present SIMC 2.0, a new secure inference model resilient to malicious clients and achieves up to $5\times$ performance improvement over the previous state-of-the-art SIMC. SIMC 2.0 complies with the underlying structure of SIMC, but designs highly optimized methods to substantially reduce the overhead of linear and non-linear layers. In short, the contributions of SIMC 2.0 are summarized as follows:

- We design a new coding method for homomorphic linear computation in an SIMD manner. It is custom-built through the insight into the complementarity between cryptographic primitives in an HE-GC based framework, where the property of secret sharing is used to convert a large number of private rotation operations to be executed in the plaintext environment. Moreover, we design a block-combined diagonal encoding method to further reduce the number of rotation operations. As a result, compared with SIMC, we reduce the complexity of rotation operations required by the matrix-vector computations from $(\log_2(\frac{n}{n_p}) + \frac{n_i n_o}{n} - 1)$ to $(l - 1)$, where l is a hyperparameter set by the server. We also present a new method for the homomorphic convolution operation with the SIMD support.
- We reduce the size of the GC in SIMC by about two thirds. As discussed above, instead of using the GC to calculate the entire ReLU function, we only encapsulate the non-linear part of ReLU into the GC. Then, we construct a lightweight

alternative protocol that takes the output of the simplified GC as input to calculate the sharing of the desired result. We exploit the authenticated shares [24] as the basis to build the lightweight alternative protocol. As a result, compared with SIMC, SIMC 2.0 reduces the communication overhead of calculating each ReLU from $2c\lambda + 4\kappa\lambda + 6\kappa^2$ to $2e\lambda + 4\kappa\lambda + 6\kappa^2 + 2\kappa$, where $e < c$ denotes the number of AND gates required in the GC.

- We demonstrate that SIMC 2.0 has the same security properties as SIMC, i.e., it is secure against the malicious client model. We prove this with theoretical analysis following the similar logic of SIMC. We use several datasets (e.g., MNIST, CIFAR-10) to conduct extensive experiments on various ML models. Our experiments show that SIMC 2.0 achieves a significant speedup by up to $17.4\times$ for linear layer computation and at least $1.3\times$ communication reduction in non-linear layer computation under different data dimensions. Meanwhile, SIMC 2.0 demonstrates an encouraging runtime boost by $2.3 \sim 4.3\times$ over SIMC on different state-of-the-art ML models (e.g., AlexNet, VGG, ResNet).

Roadmap: The remainder of this paper is organized as follows. In Section I, we review some basic concepts and introduce the scenarios and threat models involved in this paper. In Sections II – IV, we give the details of our SIMC 2.0. Performance evaluation is presented in Section V, and Section VI concludes the paper.

I. PRELIMINARIES

A. Threat Model

We consider a two-party ML inference scenario consisting of a server S_0 and a client S_1 . S_0 holds an ML model M with the private and sensitive weight W . It is considered semi-honest: it obeys the deployment procedure of ML inference, but may be curious to infer the client’s data by observing the data flow in the running process. S_1 holds the private input t . It is malicious and can arbitrarily violate the protocol specification. The model architecture NN of M is assumed to be known by both the server and the client. Our goal is to design a secure inference framework, which enables S_1 to learn the inference result of t without knowing any details about the model weight W , and S_0 knows nothing about the input t . A formal definition of the threat model is provided in Appendix A.

B. Notations

We describe some notations used in this paper. Specifically, λ and σ denote the computational and statistical security parameters. For any $n > 0$, $[n]$ denotes the set $\{1, 2, \dots, n\}$. In our SIMC 2.0, all arithmetic operations such as addition and multiplication are performed in the field \mathbb{F}_p , where p is a prime and $\kappa = \lceil \log p \rceil$. We assume that any element $x \in \mathbb{F}_p$ can be naturally mapped to the set $\{1, 2, \dots, \kappa\}$, where we use $x[i]$ to represent the i -th bit of x , i.e., $x = \sum_{i \in [\kappa]} x[i] \cdot 2^{i-1}$. For a vector \mathbf{x} and an element $\alpha \in \mathbb{F}_p$, $\alpha + \mathbf{x}$ and $\alpha \mathbf{x}$ denote the addition and multiplication of each component in \mathbf{x} with α , respectively. Given a function $f : \mathbb{F}_p \rightarrow \mathbb{F}_p$, $f(\mathbf{x})$ represents

the evaluation on f for each component in \mathbf{x} . Given two elements $x, y \in \mathbb{F}_p$, $x||y$ denotes the concatenation of x and y .

For simplicity, we assume the targeted ML architecture NN consists of alternating linear and nonlinear layers. Let the specifications of the linear layers and non-linear layers be $\mathbf{N}_1, \mathbf{N}_2, \dots, \mathbf{N}_m$ and f_1, f_2, \dots, f_{m-1} , respectively. Given an input vector \mathbf{t}_0 , the model sequentially computes $\mathbf{u}_i = \mathbf{N}_i \cdot \mathbf{t}_{i-1}$ and $\mathbf{t}_i = f_i(\mathbf{u}_i)$, where $i \in [m-1]$. As a result, we have $\mathbf{u}_m = \mathbf{N}_m \cdot \mathbf{t}_{m-1} = \text{NN}(\mathbf{t}_0)$.

C. Fully Homomorphic Encryption (FHE)

FHE is a public key encryption system that supports the evaluation of any function parsed as a polynomial in ciphertext. Informally, assuming that the message space is \mathbb{F}_p , FHE contains the following four algorithms:

- $\text{KeyGen}(1^\lambda) \rightarrow (pk, sk)$. Given the security parameter λ , KeyGen is a randomized algorithm that generates a public key pk and the corresponding secret key sk .
- $\text{Enc}(pk, t) \rightarrow c$. Given the public key pk and a message $t \in \mathbb{F}_p$ as input, Enc outputs a ciphertext c .
- $\text{Dec}(sk, c) \rightarrow t$. Given the secret key sk and a ciphertext c as input, Dec decrypts c and obtains the plaintext t .
- $\text{Eval}(pk, c_1, c_2, F) \rightarrow t$. Given the public key pk and two ciphertexts c_1, c_2 encrypting t_1, t_2 , respectively, and a function F parsed as a polynomial, Eval outputs a ciphertext c' encrypting $F(t_1, t_2)$.

We require FHE to satisfy correctness, semantic security and additive homomorphism along with function privacy¹. In addition, we use the ciphertext packing technology (CPT) [25] to accelerate the parallelism of homomorphic computation. In brief, CPT is capable of packing up to n plaintexts into one ciphertext containing n plaintext slots, thereby improving the parallelism of computation. This makes homomorphic addition and multiplication for the ciphertext equivalent to performing the same operation on every plaintext slot at once. For example, given two ciphertexts c_1 and c_2 encrypting the plaintext vectors $\mathbf{t} = (t_0, t_1, \dots, t_n)$ and $\mathbf{t}' = (t'_0, t'_1, \dots, t'_n)$ respectively, $\text{Eval}(pk, c_1, c_2, F = (a+b))$ outputs a ciphertext c encrypting the plaintext vector $\mathbf{t}'' = (t_0+t'_0, t_1+t'_1, \dots, t_n+t'_n)$.

CPT also provides a *rotation* function Rot to facilitate rotate operations between plaintexts in different plaintext slots. To be precise, given a ciphertext c encrypting a plaintext vector $\mathbf{t} = (t_0, t_1, \dots, t_n)$, $\text{Rot}(pk, c, j)$ transforms c into an encryption of $\mathbf{t}' = (t_j, t_{j+1}, \dots, t_0, \dots, t_{j-1})$, which enables the packed vector in the appropriate position to realize the correct element-wise addition and multiplication. Since the computation cost of the rotation operation in FHE is much more expensive than other operations such as homomorphic addition and multiplication, in our SIMC 2.0, we aim to design homomorphic parallel computation methods customized for

¹Informally, it means given a ciphertext c encrypting a share of ciphertext $F(c_1, c_2)$ obtained by homomorphically evaluating F , c is indistinguishable from another ciphertext c' which is a share of ciphertext $F'(c_1, c_2)$ for any other F' , even given sk .

matrix-vector multiplication and convolution, thereby minimizing the number of rotation operations incurred during execution.

D. Secret Sharing

We describe some terms used for secret sharing as follows.

- **Additive secret sharing.** Given $x \in \mathbb{F}_p$, we say a 2-of-2 additive secret sharing of x is a pair $(\langle x \rangle_0, \langle x \rangle_1) = (x - r, r) \in \mathbb{F}_p^2$ satisfying $\langle x \rangle_0 + \langle x \rangle_1 = x$, where r is randomly selected from \mathbb{F}_p . Additive secret sharing is perfectly hidden, i.e., given $\langle x \rangle_0$ or $\langle x \rangle_1$, the value of x is perfectly hidden.
- **Authenticated shares.** Given a randomly selected $\alpha \in \mathbb{F}_p$ (known as the MAC key), the authenticated share of $x \in \mathbb{F}_p$ is denoted as $\{\langle x \rangle_b, \langle \alpha x \rangle_b\}_{b \in \{0,1\}}$, where each party S_b holds $(\langle x \rangle_b, \langle \alpha x \rangle_b)$. In the fully malicious protocol, α should be shared secretly with all parties. In our client-malicious model, consistent with previous works [9], [10], α is picked uniformly by the server S_0 and secretly shared with the client S_1 . Authenticated shares provide $\lfloor \log p \rfloor$ bits of statistical security. Specifically, assuming the malicious S_1 has tampered with the share of x as $x+\beta$ by changing the shares $(\langle x \rangle_1, \langle \alpha x \rangle_1)$ to $(\langle x \rangle_1 + \beta, \langle \alpha x \rangle_1 + \beta')$, the probability of parties being authenticated to hold the share of $x+\beta$ (i.e., $\alpha x + \beta' = \alpha(x + \beta)$) is at most $2^{-\lfloor \log p \rfloor}$.
- **Authenticated Beaver's multiplicative triples.** Given a randomly selected triple $(A, B, C) \in \mathbb{F}_p^3$ satisfying $AB = C$, an authenticated Beaver's multiplicative triple denotes that S_b holds the following shares

$$\{(\langle A \rangle_b, \langle \alpha A \rangle_b), (\langle B \rangle_b, \langle \alpha B \rangle_b), (\langle C \rangle_b, \langle \alpha C \rangle_b)\}$$

for $b \in \{0, 1\}$. The process of generating triples is offline and is used to facilitate multiplication between authenticated shares. We give details of generating such triples in Figure 7 in Appendix B.

E. Oblivious Transfer

The 1-out-of-2 Oblivious Transfer (OT) [26] is denoted as OT_n , where the inputs of the sender (S_0) are two strings $s_0, s_1 \in \{0, 1\}^n$, and the input of the receiver (S_1) is a choice bit $b \in \{0, 1\}$. At the end of the OT-execution, S_1 obtains s_b while S_0 receives nothing. Succinctly, the security properties of OT_n require that 1) the receiver learns nothing but s_b and 2) the sender knows nothing about the choice b . In this paper, we require that the instance of OT_n is secure against a semi-honest sender and a malicious receiver. We use OT_n^κ to represent κ instances of OT_n . We exploit [26] to implement OT_n^κ with the communication complexity of $\kappa\lambda + 2n$ bits.

F. Garbled Circuits

A garbled scheme [27] for Boolean circuits consists of two algorithms, Garble and GCEval , defined as follows.

- $\text{Garble}(1^\lambda, C) \rightarrow (\text{GC}, \{\{\text{lab}_{i,j}^{\text{in}}\}_{i \in [n]}, \{\text{lab}_j^{\text{out}}\}\}_{j \in \{0,1\}})$. Given the security parameter λ and a Boolean circuit $C : \{0, 1\}^n \rightarrow \{0, 1\}$, the Garble function outputs a garbled circuit GC , an input set $\{\{\text{lab}_{i,j}^{\text{in}}\}_{i \in [n], j \in \{0,1\}}\}$ of labels and an output set $\{\{\text{lab}_j^{\text{out}}\}_{j \in \{0,1\}}\}$, where each label is of λ bits.

In brief, $\{\text{lab}_{i,x[i]}^{\text{in}}\}_{i \in [n]}$ represents the garbled input for any $x \in \{0,1\}^n$ and the label $\text{lab}_{C(x)}^{\text{out}}$ represents the garbled output for $C(x)$.

- $\text{GCEval}(\text{GC}, \{\text{lab}_i\}_{i \in [n]}) \rightarrow \text{lab}'$. Given the garbled circuit GC and a set of labels $\{\text{lab}_i\}_{i \in [n]}$, GCEval outputs a label lab' .

The above garbled scheme (Garble , GCEval) is required to satisfy the following properties:

- **Correctness.** GCEval is faithfully evaluated on GC and outputs $C(x)$ if the garbled x is given. Formally, for any circuit C and $x \in \{0,1\}^n$, we have

$$\text{GCEval}(\text{GC}, \{\text{lab}_{i,x[i]}^{\text{in}}\}_{i \in [n]}) \rightarrow \text{lab}_{C(x)}^{\text{out}}$$

- **Security.** For any circuit C and input $x \in \{0,1\}^n$, there exists a polynomial probability-time simulator Sim that can simulate the GC and garbled input of x generated by Garble under real execution, *i.e.*, $(\text{GC}, \{\text{lab}_{i,x[i]}^{\text{in}}\}_{i \in [n]}) \approx \text{Sim}(1^\lambda, C)$, where \approx indicates computational indistinguishability of two distributions $(\text{GC}, \{\text{lab}_{i,x[i]}^{\text{in}}\}_{i \in [n]})$ and $\text{Sim}(1^\lambda, C)$.
- **Authenticity.** It is infeasible to guess the output label of $1 - C(x)$ given the garbled input of x and GC. Formally, for any circuit C and $x \in \{0,1\}^n$, we have $(\text{lab}_{1-C(x)}^{\text{out}} | \text{GC}, \{\text{lab}_{i,x[i]}^{\text{in}}\}_{i \in [n]}) \approx U_\lambda$, where U_λ represents the uniform distribution on the set $\{0,1\}^n$.

Note that the garbled scheme described above can be naturally extended to the case with multiple garbled outputs. We also utilize state-of-the-art optimization strategies, including point-and-permute, free-XOR and half-gates [28] to construct the garbled circuit. We provide a high-level description of performing a secure two-party computation with GC: assuming that a semi-honest server S_0 and a malicious client S_1 hold private inputs x and y , respectively. Both parties evaluate $C(x, y)$ on GC as follows. S_0 first garbles the circuit C to learn GC and garbled labels about the input and output of GC. Then, both parties invoke the OT functionality, where the sender S_0 inputs garbled labels corresponding to the input wires of S_1 , while the receiver S_1 inputs y to obtain garbled inputs of y . S_0 additionally sends the garbled input of x , GC and a pair of ciphertexts for every output wire w of C to S_1 . As a result, S_1 evaluates GC to learn the garbled output of $C(x, y)$ with the received garbled input about x and y . From the garbled output and the pair of ciphertexts given for each output wire, S_1 finally gets $C(x, y)$. S_1 sends $C(x, y)$ along with the hash of the garbled output to S_0 for verification. S_0 accepts it if the hash value corresponds to $C(x, y)$.

II. LINEAR LAYER OPTIMIZATION

We start by describing the secure execution of linear layers in SIMC. To be precise, SIMC designs two protocols (**InitLin** and **Lin**) to securely perform linear layer operations, as shown in **Figures 8** and **9** in Appendix C. We observe that the most computationally intensive operations in **InitLin** and **Lin** are homomorphically computing $\mathbf{N} \cdot \mathbf{t}$ and $\alpha \mathbf{N} \cdot \mathbf{t}$ (including matrix-vector multiplication in FC layers and convolution operations in convolution layers), where \mathbf{N} is a plaintext

weight matrix held by the server, and \mathbf{t} (will be encrypted as $[\mathbf{t}]_c$) is the input held by the client.

We focus on the optimization of matrix-vector parallel multiplication. More specifically, we consider an FC layer with n_i inputs and n_o outputs, *i.e.*, $\mathbf{N} \in \mathbb{F}_p^{n_o \times n_i}$. The client's input is a ciphertext vector $\mathbf{t} \in \mathbb{F}_p^{n_i}$. n is the number of slots in a ciphertext. We first describe a naive approach to parallelize homomorphic multiplication of $\mathbf{N} \cdot \mathbf{t}$, followed by a state-of-the-art method proposed by GAZELLE [20]. Finally we introduce our proposed scheme that substantially reduces the computation cost of matrix-vector multiplication.

A. Naive Method

The naive method of matrix-vector multiplication is shown in **Figure 1**, where \mathbf{N} is the $n_o \times n_i$ dimensional plaintext matrix held by the server and $[\mathbf{t}]_c$ is the encryption of the client's input vector. The server encodes each row of the matrix into a separate plaintext vector (Step (a) in **Figure 1**), where each encoded vector is of length n (including zero-padding if necessary). We denote these encoded plaintext vectors as $\mathbf{N}_0, \mathbf{N}_1, \dots, \mathbf{N}_{n_o-1}$. For example, there are four vectors in **Figure 1**, namely $\mathbf{N}_0, \mathbf{N}_1, \mathbf{N}_2$, and \mathbf{N}_3 .

The purpose of the server is to homomorphically compute the dot product of the plaintext \mathbf{N} and the ciphertext $[\mathbf{t}]_c$. Let ScMult be the scalar multiplication of a plaintext and a ciphertext in HE. The server first uses ScMult to compute the element-wise multiplication of \mathbf{N}_i and $[\mathbf{t}]_c$. As a result, the server gets $[\mathbf{v}_i]_c = [\mathbf{N}_i \odot \mathbf{t}]_c$ (Step (b) in **Figure 1**). We observe that the sum of all elements in $[\mathbf{v}_i]_c$ is the i -th element of the desired dot product of \mathbf{N} and $[\mathbf{t}]_c$. Since there is no direct way to obtain this sum in HE, we rely on the rotation operation to do it. To be precise, as shown in Step (c) in **Figure 1**, $[\mathbf{v}_i]_c$ is first rotated by permuting $\frac{n_i}{2}$ positions such that the first $\frac{n_i}{2}$ entries of the rotated $[\mathbf{v}_i]_c$ are the second $\frac{n_i}{2}$ entries of the original $[\mathbf{v}_i]_c$. The server then performs element-wise addition on the original $[\mathbf{v}_i]_c$ and the rotated one homomorphically, which derives a ciphertext whose sum of the first $\frac{n_i}{2}$ entries is actually the desired result. The server iteratively performs the above rotation operation for $\log_2 n_i$ times. Each time it operates on the ciphertext derived from the previous iteration. The server finally gets the ciphertext whose first entry is the i -th element of \mathbf{Nt} . By executing this procedure for each $[\mathbf{v}_i]_c$, *i.e.*, $[\mathbf{v}_0]_c, [\mathbf{v}_1]_c, [\mathbf{v}_2]_c$, and $[\mathbf{v}_3]_c$ in **Figure 1**, the server obtains n_o ciphertexts. Consistently, the first entries of these ciphertexts correspond to the elements in \mathbf{Nt} .

We now analyze the complexity of the above matrix-vector multiplication. We consider the process starting with the server receiving the ciphertext (*i.e.*, $[\mathbf{t}]_c$) from the client until it obtains the ciphertext (*i.e.*, n_o ciphertexts) to be shared². There are totally n_o scalar multiplication operations (*i.e.*, ScMult), $n_o \log_2 n_i$ rotation operations and $n_o \log_2 n_i$ addition operations. It produces n_o output ciphertexts, each containing

²In the neural network inference process with HE-GC as the underlying structure, the ciphertext generated in the linear phase will be securely shared between the client and the server, and used as the input of the subsequent GC-based nonlinear function. Readers can refer to [9], [10], [11] for more details.

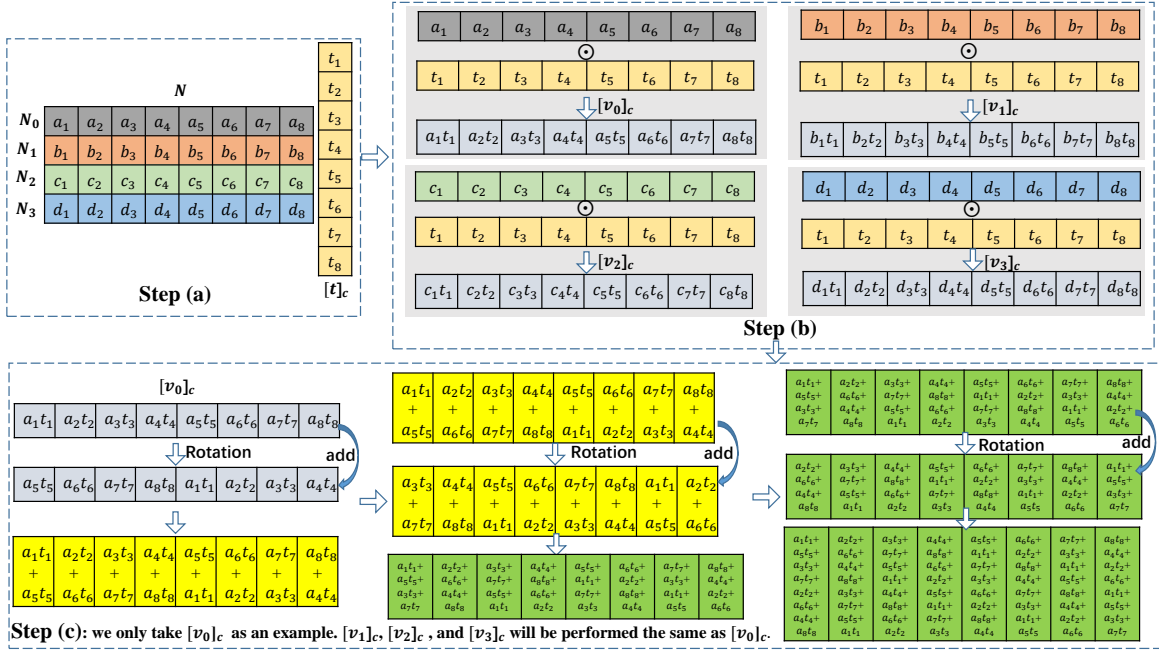


Fig. 1: Naive matrix-vector multiplication

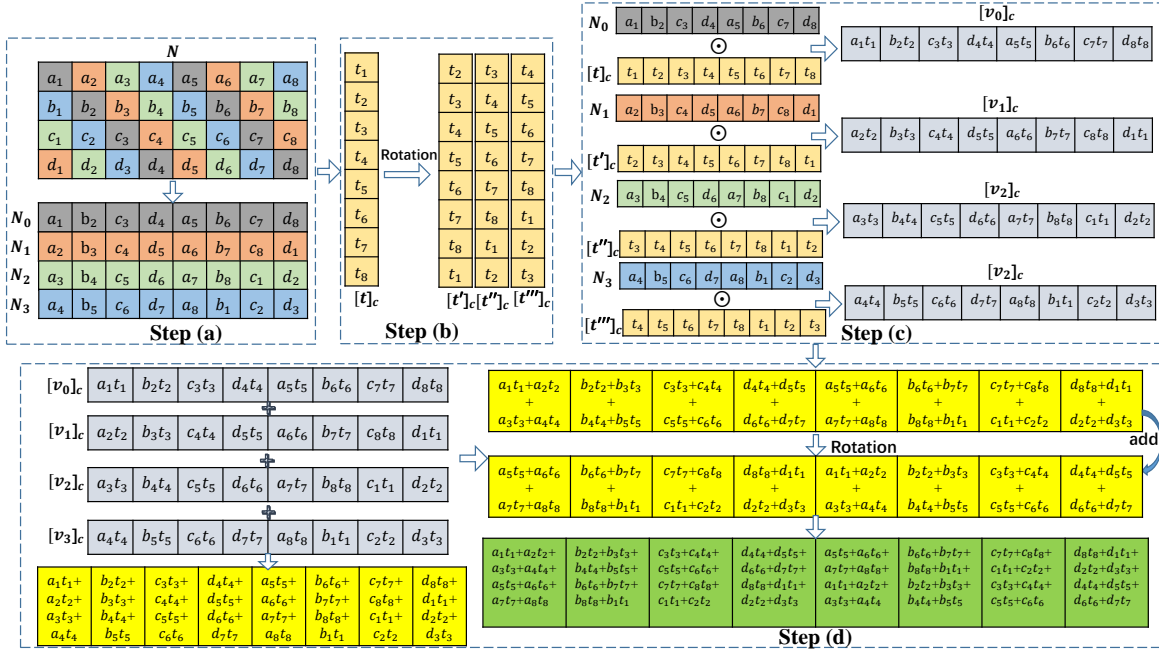


Fig. 2: Hybrid matrix-vector multiplication

an element in Nt . Such naive use of the ciphertext space inevitably incurs inefficiencies for linear computations.

B. Hybrid Method (GAZELLE)

In order to fully utilize n slots and substantially reduce the computation complexity, Juvekar *et al.* [20] propose GAZELLE, a state-of-the-art hybrid method customized for the HE-GC based secure inference. It has been integrated into some advanced solutions such as DELPHI [15] and EzPC[22]. The core idea of GAZELLE also inspires the design of MUSE

and SIMC, as they inherit DELPHI's optimization strategy for HE-based linear operations. GAZELLE is actually a variant of diagonal encoding [25], which exploits the fact that n_o is usually much smaller than n_i in the FC layer. Based on this, GAZELLE shows that the most expensive rotation operation is a function of n_o rather than n_i , thus speeding up the calculation of the FC layer.

The basic idea of GAZELLE is shown in **Figure 2**. The server encodes the matrix N diagonally into a vector of n_o plaintexts. For example, as shown in **Step (a)** in **Figure 2**, the

first plaintext vector \mathbf{N}_0 consists of gray elements in matrix \mathbf{N} , *i.e.*, $(a_1, b_2, c_3, d_4, a_5, b_6, c_7, d_8)$. The second plaintext vector \mathbf{N}_1 consists of orange elements $(a_2, b_3, c_4, d_5, a_6, b_7, c_8, d_1)$. The composition of \mathbf{N}_2 and \mathbf{N}_3 is analogous. Note that the meaning of \mathbf{N}_0 to \mathbf{N}_3 in the hybrid approach is different from the previous naive approach in Section II-A.

For $i = 1$ to $n_o - 1$, the server rotates $[\mathbf{t}]_c$ by i positions, as shown in Step (b) in **Figure 2**. Afterwards, ScMult is used to perform the element-wise multiplication of \mathbf{N}_i and the corresponding ciphertext. For example, as shown in Step (c) in **Figure 2**, \mathbf{N}_0 is multiplied by the ciphertext $[\mathbf{t}]_c$, while \mathbf{N}_1 is multiplied by $[\mathbf{t}']_c$, and so on. As a result, the server obtains n_o multiplied ciphertexts, $\{[\mathbf{v}_i]_c\}$. The server receives four ciphertexts $\{[\mathbf{v}_0]_c, [\mathbf{v}_1]_c, [\mathbf{v}_2]_c, [\mathbf{v}_3]_c\}$, whose elements are all part of the desired dot product. Then, the server sums all ciphertexts $[\mathbf{v}_i]_c$ (Step (d) in **Figure 2**) in an element-wise way to form a new ciphertext. At this point, the server performs rotation operations similar to the naive approach, *i.e.*, iteratively performing $\log_2 \frac{n_i}{n_o}$ rotations followed by addition to obtain a final single ciphertext. The first n_o entries of this ciphertext correspond to the n_o ciphertext elements of \mathbf{Nt} .

To further reduce the computation cost, GAZELLE proposes combining multiple copies of \mathbf{t} into a single ciphertext (called $[\mathbf{t}_{\text{pack}}]_c$), since the number n of slots in a single ciphertext is usually larger than the dimension n_i of the input vector. As a result, $[\mathbf{t}_{\text{pack}}]_c$ has $\frac{n}{n_i}$ copies of \mathbf{t} so that the server can perform ScMult operations on $[\mathbf{t}_{\text{pack}}]_c$ with $\frac{n}{n_i}$ encoded vectors at one time. This causes the server to get $\frac{n_i n_o}{n}$ ciphertexts instead of n_o ciphertexts, which results in a single ciphertext holding $\frac{n}{n_o}$ rather than $\frac{n_i}{n_o}$ blocks. Finally, the server iteratively performs $\log_2 \frac{n}{n_o}$ rotations followed by addition to obtain a single final ciphertext, where the first n_o entries in this ciphertext correspond to the n_o ciphertext elements of \mathbf{Nt} .

In terms of complexity, GAZELLE requires $\frac{n_i n_o}{n}$ scalar multiplications, $\log_2 \frac{n}{n_o} + \frac{n_i n_o}{n} - 1$ rotations, and $\log_2 \frac{n}{n_o} + \frac{n_i n_o}{n} - 1$ additions. It outputs only one ciphertext, which greatly improves the efficiency and utilization of slots over the naive approach.

C. Our Method

In the above hybrid method, the rotation operation comes from two parts: rotations required for the client's encrypted input (Step (b) in **Figure 2**) and the subsequent rotations followed by addition involved in obtaining the final matrix-vector result (Step (d) in **Figure 2**). Therefore, our approach is motivated by two observations in order to substantially reduce the number of rotation operations incurred by these two aspects. First, we divide the server's original $n_o \times n_i$ -dimensional weight matrix \mathbf{N} into multiple sub-matrices, and calculate each sub-matrix separately (explained later based on **Figure 3**). This can effectively reduce the number of rotations for the client's ciphertext $[\mathbf{t}]_c$ from $n_o - 1$ to $l - 1$, where l is a hyperparameter set by the server.

Second, for the rotations followed by addition (Step (d) in **Figure 2**), we claim that they are actually not necessary. This is determined by the characteristics of the HE-GC based secure inference framework. To be precise, the ciphertexts

output from the FC layer will be secretly shared with the client and server, and used as the input of the next non-linear layer function. As the shares are in plaintext, we can completely convert the rotation followed by addition to be performed under plaintext. This will significantly reduce the computation complexity. For example, given a 16×256 -dimensional matrix and a vector of length 256, our experiments indicate at least a $3.5 \times$ speedup compared to the hybrid method (see more details in Section V).

Figure 3 illustrates our matrix-vector calculation procedure. Specifically, we first split the matrix \mathbf{N} into multiple sub-matrices. As shown in Step (a) in **Figure 3**, for simplicity, we take the first $l = 2$ rows (*i.e.*, \mathbf{N}_0 and \mathbf{N}_1) of \mathbf{N} as a sub-matrix, thus \mathbf{N}_2 and \mathbf{N}_3 form another sub-matrix. Then, we exploit the diagonal method to arrange the $1 \times (n_i/l)$ sized sub-matrices of \mathbf{N} as a sub-matrix, which results in two new sub-matrices. For subsequent ciphertext parallel computation, we need to sequentially perform $l - 1$ rotations of the client's input $[\mathbf{t}]_c$, starting from moving the $(n_i/l + 1)$ -th entry to the first entry. In Step (b) in **Figure 3**, $[\mathbf{t}]_c$ is rotated into $[\mathbf{t}']_c$, where the first entry of $[\mathbf{t}']_c$ is the $(8/2 + 1) = 5$ -th entry of $[\mathbf{t}]_c$.

ScMult is further used to perform the element-wise multiplication of \mathbf{N}_i and the corresponding ciphertext. For example, as shown in Step (c) in **Figure 3**, \mathbf{N}_0 is multiplied by the ciphertext $[\mathbf{t}]_c$, while \mathbf{N}_1 is multiplied by $[\mathbf{t}']_c$. \mathbf{N}_2 and \mathbf{N}_3 are operated similarly. As a result, the server obtains n_o multiplied ciphertexts $\{[\mathbf{v}_i]_c\}$, which can be divided into l independent ciphertext pairs. We can observe that the server gets two independent ciphertext pairs, *i.e.*, $\{[\mathbf{v}_0]_c, [\mathbf{v}_1]_c\}$ and $\{[\mathbf{v}_2]_c, [\mathbf{v}_3]_c\}$. For each individual set of ciphertexts, the server adds up all ciphertexts in that set in an element-wise way, thus forming l new ciphertexts (yellow boxes in Step (d) in **Figure 3**).

Until now, a natural approach is to perform rotation followed by addition on each ciphertext, as in the hybrid approach. This will take a total of n_i/l rotations and derive n_o/l ciphertexts. However, we argue that such ciphertext operations are not necessary and can be converted to plaintext to be performed. Our key insight is that the ciphertext result of the FC layer will be secretly shared with the client and server. Therefore, we require the server to generate random vectors (*i.e.*, $\{\mathbf{r}_i\}_{i \in [8]}$ and $\{\mathbf{q}_i\}_{i \in [8]}$ in Step (d) of **Figure 3**), and then subtract the random vectors from the corresponding ciphertexts. The server returns the subtracted ciphertexts to the client, which decrypts them and executes n_i/l plaintext rotation followed by addition operations on them to obtain its share. Similarly, the server gets its share by executing n_i/l plaintext rotation followed by addition operations on its random vectors. Compared to GAZELLE, our method only needs to perform $l - 1$ rotations on the client's input, and does not require any rotations subsequently. This significantly improves the performance of matrix-vector computations.

We further reduce the computation cost by packing multiple copies of \mathbf{t} into a single ciphertext (called $[\mathbf{t}_{\text{pack}}]_c$). As a result, $[\mathbf{t}_{\text{pack}}]_c$ has $\frac{n}{n_i}$ copies of \mathbf{t} so that the server can perform ScMult operations on $[\mathbf{t}_{\text{pack}}]_c$ with $\frac{n}{n_i}$ encoded vectors at one time. The computation cost of our method is

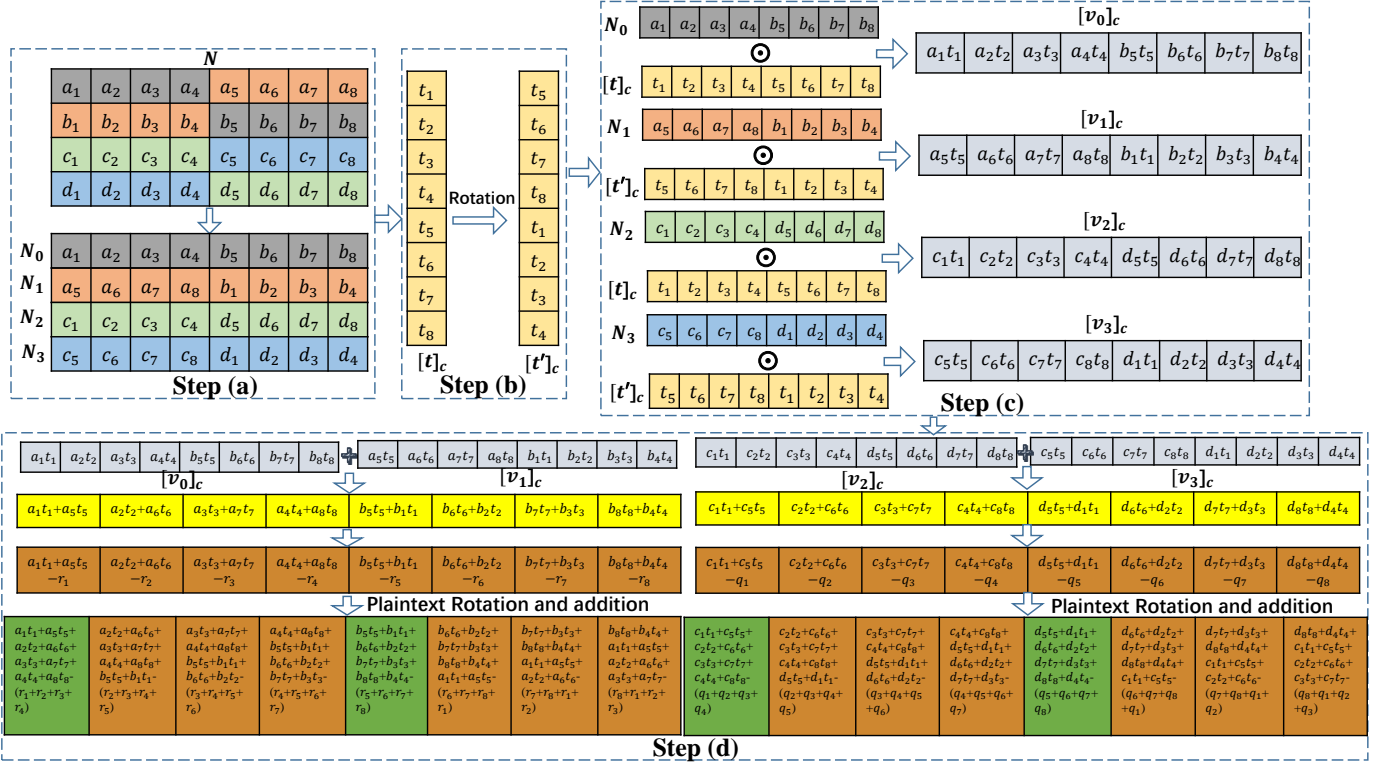


Fig. 3: Our matrix-vector multiplication algorithm

$\frac{n_i n_o}{n}$ homomorphic multiplication operations, $l - 1$ rotation operations, and $\frac{n_i n_o}{n} - 1$ homomorphic addition operations. It outputs $n_i \cdot n_o / (l \cdot n)$ ciphertexts.

Remark 3.1. Table I shows the comparison of our method with existing approaches in computation complexity. It is obvious that our method has better complexity, especially for rotation operations. Note that GALA [16] also designs an improved version of GAZELLE [20] for matrix-vector multiplication, which has the computation complexity of $(\frac{n_i n_o}{n} - 1)$ for rotation operations. However, GALA is specially customized for secure inference under the *semi-honest adversary model*. It is not clear whether it can be smoothly transferred to the *client-malicious adversary model*. Moreover, our method still outperforms GALA in the computation complexity.

TABLE I: Computation complexity of each method

| Method | #Rotation | #ScMul | #Add |
|------------|--|---------------------|--|
| Naive | $\frac{n_o \log_2 n_i}{n}$ | $\frac{n_o}{n}$ | $\frac{n_o \log_2 n_i}{n}$ |
| Hybrid | $\log_2 \frac{n}{n_o} + \frac{n_i n_o}{n} - 1$ | $\frac{n_i n_o}{n}$ | $\log_2 \frac{n}{n_o} + \frac{n_i n_o}{n} - 1$ |
| Our method | $l - 1$ | $\frac{n_i n_o}{n}$ | $\frac{n_i n_o}{n} - 1$ |

Remark 3.2. We also describe the optimization of convolution operations for linear layers. In brief, we assume that the server has c_o plaintext kernels of size $k_w \times k_h \times c_i$, and the ciphertext input sent by the client to the server is c_i kernels of size $u_w \times u_h$. The server is required to perform homomorphic convolution operations between the ciphertext input and its own plaintext kernel to obtain the ciphertext output. To improve the parallel processing capabilities, GAZELLE proposes to pack the input data of c_n channels into one ciphertext, and requires a total of $\frac{c_i(k_w k_h - 1)}{c_n}$ rotation operations to achieve

convolution. We present an improved solution over GAZELLE to execute convolution operations. We design strategies to significantly reduce the number of rotation operations involved in computing the convolution between each of the $\frac{c_o c_i}{c_n}$ blocks and the corresponding input channels (see Appendix D). As a result, our method reduces the computation complexity with respect to rotations by a factor of $\frac{c_i}{c_n}$ compared to GAZELLE. Readers can refer to Appendix D for more details.

III. NONLINEAR LAYER OPTIMIZATION

In this section, we describe our proposed optimization method for non-linear layers. We focus on the secure computation of the activation function ReLU, one of the most popular functions in non-linear layers of modern DNNs. As shown in Section II, the output of each linear layer will be securely shared with the server and client (Figures 8 and 9 in Appendix C), and used as the input of the next non-linear layer to obtain authenticated shares of the output of the non-linear layer. Specifically, assume the output of a linear layer is $\mathbf{u} = \langle \mathbf{u} \rangle_0 + \langle \mathbf{u} \rangle_1$, where $\langle \mathbf{u} \rangle_0$ and $\langle \mathbf{u} \rangle_1$ are the shares held by the server and the client, respectively. Then the functionality of the next nonlinear layer is shown in Figure 4. At the high level, the main difference between our method and SIMC comes from parsing ReLU as $f(\mathbf{u}) = \mathbf{u} \cdot \text{sign}(\mathbf{u})$ and encapsulating only the non-linear part ($\text{sign}(\mathbf{u})$) into the GC. The sign function $\text{sign}(t)$ equals 1 if $t \geq 0$ and 0 otherwise. In this way, we can reduce the original GC size by about two-thirds, thereby further reducing the computation and communication costs incurred by running non-linear layers.

Similar to SIMC, our method can be divided into four phases: Garbled Circuit phase, Authentication phase 1, Local

Function $f : \mathbb{F}_p \rightarrow \mathbb{F}_p$.
Input: S_0 holds $\langle \mathbf{u} \rangle_0 \in \mathbb{F}_p$ and a MAC key α uniformly chosen from \mathbb{F}_p . S_1 holds $\langle \mathbf{u} \rangle_1 \in \mathbb{F}_p$.
Output: S_b obtains $\{(\langle \alpha \rangle_b, \langle f(\mathbf{u}) \rangle_b, \langle \alpha f(\mathbf{u}) \rangle_b)\}$ for $b \in \{0, 1\}$.

Figure 4: Functionality of the nonlinear layer

Computation phase, and Authentication phase 2. Assume the server's (S_0) input is $(\langle \mathbf{u} \rangle_0, \alpha)$ and the client's (S_1) input is $(\langle \mathbf{u} \rangle_1)$. We provide a high-level view of the protocol. **Figure 5** gives a detailed technical description.

Garbled Circuit Phase. SIMC uses the GC to calculate every bit of \mathbf{u} and $ReLU(\mathbf{u})$, instead of directly calculating these values. This is efficient, since it avoids incurring a large number of multiplication operations in the GC. Our method follows a similar logic, but instead of computing $ReLU(\mathbf{u})$, we compute every bit of $sign(\mathbf{u})$. In this phase we can reduce the original GC size by about two-thirds. To achieve this, S_0 first constructs a garbled circuit for $booln^f$, where the input of the circuit is the share of \mathbf{u} and its output is $(\mathbf{u}, sign(\mathbf{u}))$. S_1 evaluates this garbled circuit on $\langle \mathbf{u} \rangle_0$ and $\langle \mathbf{u} \rangle_1$ once the correct input labels are obtained through the OT protocol. At the end, S_1 learns the set of output labels for the bits of \mathbf{u} and $sign(\mathbf{u})$.

Authentication Phase 1. In the previous phase S_1 obtains the garbled output labels for each bit of \mathbf{u} and $sign(\mathbf{u})$, denoted as $\mathbf{u}[i]$ and $sign(\mathbf{u})[i]$, respectively. The goal of this phase is to compute the shares of $\alpha \mathbf{u}[i]$, $sign(\mathbf{u})[i]$, and $\alpha sign(\mathbf{u})[i]$. We take $\alpha \mathbf{u}[i]$ as an example to briefly describe the procedure. Specifically, we observe that the shares of $\alpha \mathbf{u}[i]$ are either shares 0 or α , depending on whether $\mathbf{u}[i]$ is 0 or 1. Also, the output of the GC contains two output labels corresponding to each $\mathbf{u}[i]$ (each one for $\mathbf{u}[i] = 0$ and 1). Therefore, we denote these labels as $lab_{i,0}^{out}$ and $lab_{i,1}^{out}$ for $\mathbf{u}[i] = 0$ and $\mathbf{u}[i] = 1$, respectively. To calculate the shares of $\alpha \mathbf{u}[i]$, S_0 chooses a random number $\tau_i \in \mathbb{F}_p$ and converts it to $lab_{i,0}^{out}$. Similarly, $\tau_i + \alpha$ is converted to $lab_{i,1}^{out}$. S_0 sends the two ciphertexts to S_1 , and sets its share of $\alpha \mathbf{u}[i]$ as $-\tau_i$. Since S_1 has obtained $lab_{i,\mathbf{u}[i]}^{out}$ in the previous phase, it can obviously decrypt one of the two ciphertexts to obtain its share for $\alpha \mathbf{u}[i]$. Computing the share of $\alpha sign(\mathbf{u})[i]$ and $sign(\mathbf{u})[i]$ follows a similar method using the output labels for $sign(\mathbf{u})$.

Local Computation Phase. Given the shares of $\alpha \mathbf{u}[i]$, $sign(\mathbf{u})[i]$, and $\alpha sign(\mathbf{u})[i]$, this phase locally calculates the shares of $\alpha \mathbf{u}$, $sign(\mathbf{u})$, and $\alpha sign(\mathbf{u})$. Taking $\alpha \mathbf{u}$ as an example, as shown in **Figure 5**, each party locally multiplies $\alpha \mathbf{u}[i]$ and 2^{i-1} and then sums these results to get the share on $\alpha \mathbf{u}$. The shares of $sign(\mathbf{u})$ and $\alpha sign(\mathbf{u})$ are calculated in a similar way.

Authentication Phase 2. This phase calculates the shares of $f(\mathbf{u}) = \mathbf{u}sign(\mathbf{u})$, and $\alpha f(\mathbf{u})$. Since each party holds the authenticated shares of \mathbf{u} and $sign(\mathbf{u})$, it is easy to compute the authenticated shares of $f(\mathbf{u})$ for each party (see **Figure 5**).

Remark 4.1. As described above, we reduce the size of the GC in SIMC by about two thirds. Therefore, instead of using the GC to calculate the entire ReLU function, we only encapsulate the non-linear part of ReLU into the GC. Then, we construct a lightweight alternative protocol that takes the output of the

simplified GC as input to calculate the shares of the desired result. Therefore, compared with SIMC, SIMC 2.0 reduces the communication overhead of calculating each ReLU from $2c\lambda + 4\kappa\lambda + 6\kappa^2$ to $2e\lambda + 4\kappa\lambda + 6\kappa^2 + 2\kappa$, where $e < c$ denotes the number of AND gates required in the GC and satisfies $(c - e > \kappa)$. Also, we experimentally demonstrate that this simplified GC improves the running efficiency by one third compared to the original one.

Remark 4.2. Our method can be easily extended to other non-linear functions, such as Maxpool. We follow the same idea to compute all the shares of Maxpool's output, where we construct a Boolean circuit for Maxpool that feeds multiple inputs $(\mathbf{u}_1, \mathbf{u}_2, \dots, \mathbf{u}_\kappa)$, and outputs the reconstructed $(\mathbf{u}_1, \mathbf{u}_2, \dots, \mathbf{u}_\kappa)$ and $f(\mathbf{u}_1, \mathbf{u}_2, \dots, \mathbf{u}_\kappa)$.

Correctness. We analyze the correctness of our protocol in **Figure 5** as follows. Based on the correctness of OT_{λ}^{κ} , the client S_1 holds $\{lab_{i,\langle \mathbf{u} \rangle_1}^{in} = lab_{i,\langle \mathbf{u} \rangle_1}^{in}\}_{i \in \{\kappa+1, \dots, 2\kappa\}}$. Since for $i \in [\kappa]$, $\{lab_{i,\langle \mathbf{u} \rangle_0}^{in} = lab_{i,\langle \mathbf{u} \rangle_0}^{in}\}_{i \in [\kappa]}$, we can get $lab_{i,\langle \mathbf{u} \rangle_1}^{out} = lab_{i,\langle \mathbf{u} \rangle_0}^{out}$ and $lab_{i+\kappa,\langle \mathbf{u} \rangle_1}^{out} = lab_{i+\kappa,\langle \mathbf{u} \rangle_0}^{out}$, with the correctness of (Garble, GCEval) for circuit $booln^f$. Therefore, for $i \in [k]$, we have $\xi_i || \zeta_i = \xi_{i,\mathbf{u}[i]} || \zeta_{i,\mathbf{u}[i]}$ and $\xi_{i+\kappa} || \zeta_{i+\kappa} = \xi_{i+\kappa,sign(\mathbf{u})[i]} || \zeta_{i+\kappa,sign(\mathbf{u})[i]}$. We also have $c_i = ct_{i,\xi_i,\mathbf{u}[i]} \oplus \text{Trun}_{\kappa}(\zeta_{i,\mathbf{u}[i]}) = \tau_{i,\mathbf{u}[i]}$ and $(d_i || e_i) = \hat{c}_{i,\xi_{i+\kappa},sign(\mathbf{u})[i]} \oplus \text{Trun}_{2\kappa}(\zeta_{i+\kappa,sign(\mathbf{u})[i]}) = \rho_{i,sign(\mathbf{u})[i]} || \sigma_{i,sign(\mathbf{u})[i]}$. Based on these, we have

- $g_1 = \sum_{i \in [\kappa]} (c_i - \tau_{i,0}) 2^{i-1} = \sum_{i \in [\kappa]} \alpha (\mathbf{u}[i]) 2^{i-1} = \alpha \mathbf{u}$.
- $g_2 = \sum_{i \in [\kappa]} (d_i - \rho_{i,0}) 2^{i-1} = \sum_{i \in [\kappa]} (sign(\mathbf{u})[i]) 2^{i-1} = sign(\mathbf{u})$.
- $g_3 = \sum_{i \in [\kappa]} (e_i - \sigma_{i,0}) 2^{i-1} = \sum_{i \in [\kappa]} \alpha (sign(\mathbf{u})[i]) 2^{i-1} = \alpha sign(\mathbf{u})$.

Since each party holds the authenticated shares of \mathbf{u} and $sign(\mathbf{u})$, we can easily compute the shares of $f(\mathbf{u}) = \mathbf{u}sign(\mathbf{u})$, and $\alpha f(\mathbf{u})$. This concludes the correctness proof.

Security. Our protocol for non-linear layers has the same security properties as SIMC, *i.e.*, it is secure against the malicious client model. We provide the following theorem and prove it in Appendix E following the similar logic of SIMC.

Theorem 1. *Let (Garble, GCEval) be a garbling scheme with the properties defined in Section I-F. Authenticated shares have the properties defined in Section I-D. Then our protocol for non-linear layers is secure against any malicious adversary A corrupting the client S_1 .*

Proof. Please refer to Appendix E. □

IV. SECURE INFERENCE

During inference, the server S_0 's input is the weights of all linear layer, *i.e.*, $\mathbf{N}_1, \dots, \mathbf{N}_m$ while the input of S_1 is \mathbf{t} . The goal of our secure inference protocol π_{inf} is to learn $NN(\mathbf{t}_0)$ for the client S_1 . Given a trained neural network consisted of linear layers and non-linear layers, SIMC 2.0 utilizes the HE-GC-based techniques as the underlying architecture to perform secure inference, where linear operations (including matrix multiplication and convolution functions) are performed with

Preamble: To compute the ReLU function $f : \mathbb{F}_p \rightarrow \mathbb{F}_p$, we consider a Boolean circuit $booln^f$ that takes the share of \mathbf{u} as input and outputs $(\mathbf{u}, f(\mathbf{u}))$. In addition, we define a truncation function $\mathbf{Trun}_h : \{0, 1\}^\lambda \rightarrow \{0, 1\}^h$, which outputs the last h bits of the input, where λ satisfies $\lambda \geq 2\kappa$.

Input: S_0 holds $\langle \mathbf{u} \rangle_0 \in \mathbb{F}_p$ and a MAC key α uniformly chosen from \mathbb{F}_p . S_1 holds $\langle \mathbf{u} \rangle_1 \in \mathbb{F}_p$.

Output: S_b obtains $\{(\langle \alpha \mathbf{u} \rangle_b, \langle f(\mathbf{u}) \rangle_b, \langle \alpha f(\mathbf{u}) \rangle_b)\}$ for $b \in \{0, 1\}$.

Protocol:

1. Garbled Circuit Phase:

- S_0 computes $\mathbf{Garble}(1^\lambda, booln^f) \rightarrow (\mathbf{GC}, \{\{\mathbf{lab}_{i,j}^{in}\}_{i \in [2\kappa]}, \{\mathbf{lab}_{i,j}^{out}\}_{i \in [2\kappa], j \in \{0,1\}}\})$. Given the security parameter λ and a boolean circuit $booln^f$, \mathbf{Garble} outputs a garbled circuit \mathbf{GC} , an input set $\{\mathbf{lab}_{i,j}^{in}\}_{i \in [2\kappa], j \in \{0,1\}}$ of labels and an output set $\{\mathbf{lab}_{i,j}^{out}\}_{i \in [2\kappa], j \in \{0,1\}}$, where each label is of λ -bits.
- S_0 (as the sender) and S_1 (as the receiver) invoke the $\mathbf{OT}_\lambda^\kappa$ (see Section I-E), where S_0 's inputs are $\{\mathbf{lab}_{i,0}^{in}, \mathbf{lab}_{i,1}^{in}\}_{i \in \{\kappa+1, \dots, 2\kappa\}}$ while S_1 's input is $\langle \mathbf{u} \rangle_1$. As a result, S_1 obtains $\{\mathbf{lab}_i^{in}\}_{i \in \{\kappa+1, \dots, 2\kappa\}}$. In addition, S_0 sends the garbled circuit \mathbf{GC} and its garbled inputs $\{\{\mathbf{lab}_i^{in} = \mathbf{lab}_{i, \langle \mathbf{u} \rangle_0 [i]}\}_{i \in [\kappa]}\}$ to S_1 .
- Given the \mathbf{GC} and the garbled inputs $\{\mathbf{lab}_i^{in}\}_{i \in [2\kappa]}$, S_1 computes $\mathbf{GCEval}(\mathbf{GC}, \{\mathbf{lab}_i^{in}\}_{i \in [2\kappa]}) \rightarrow \{\mathbf{lab}_i^{out}\}_{i \in [2\kappa]}$.

2. Authentication Phase 1:

- For every $i \in [\kappa]$, S_0 randomly selects $\rho_{i,0}$, $\sigma_{i,0}$ and $\tau_{i,0} \in \mathbb{F}_p$ and sets $(\rho_{i,1}, \sigma_{i,1}, \tau_{i,1}) = (1 + \rho_{i,0}, \alpha + \sigma_{i,0}, \alpha + \tau_{i,0})$.
- For every $i \in [2\kappa]$ and $j \in \{0, 1\}$, S_0 parses $\{\mathbf{lab}_{i,j}^{out}\}$ as $\xi_{i,j} || \zeta_{i,j}$ where $\xi_{i,j} \in \{0, 1\}$ and $\zeta_{i,j} \in \{0, 1\}^{\lambda-1}$.
- For every $i \in [\kappa]$ and $j \in \{0, 1\}$, S_0 sends $ct_{i,\xi_{i,j}}$ and $\hat{ct}_{i,\xi_{i+\kappa,j}}$ to S_1 , where $ct_{i,\xi_{i,j}} = \tau_{i,j} \oplus \mathbf{Trun}_\kappa(\zeta_{i,j})$ and $\hat{ct}_{i,\xi_{i+\kappa,j}} = (\rho_{i,j} || \sigma_{i,j}) \oplus \mathbf{Trun}_\kappa(\zeta_{i+\kappa,j})$.
- For every $i \in [2\kappa]$, S_1 parses \mathbf{lab}_i^{out} as $\tilde{\xi}_i || \tilde{\zeta}_i$ where $\tilde{\xi}_i \in \{0, 1\}$ and $\tilde{\zeta}_i \in \{0, 1\}^{\lambda-1}$.
- For every $i \in [\kappa]$, S_1 computes $c_i = ct_{i,\tilde{\xi}_i} \oplus \mathbf{Trun}_\kappa(\tilde{\zeta}_i)$ and $(d_i || e_i) = \hat{ct}_{i,\tilde{\xi}_{i+\kappa}} \oplus \mathbf{Trun}_{2\kappa}(\tilde{\zeta}_{i+\kappa})$.

3. Local Computation Phase:

- S_0 outputs $\langle g_1 \rangle_0 = (-\sum_{i \in [\kappa]} \tau_{i,0} 2^{i-1})$, $\langle g_2 \rangle_0 = (-\sum_{i \in [\kappa]} \rho_{i,0} 2^{i-1})$ and $\langle g_3 \rangle_0 = (-\sum_{i \in [\kappa]} \sigma_{i,0} 2^{i-1})$.
- S_1 outputs $\langle g_1 \rangle_1 = (\sum_{i \in [\kappa]} c_i 2^{i-1})$, $\langle g_2 \rangle_1 = (\sum_{i \in [\kappa]} d_i 2^{i-1})$ and $\langle g_3 \rangle_1 = (\sum_{i \in [\kappa]} e_i 2^{i-1})$.

4. Authentication Phase 2:

- $S_b, b \in \{0, 1\}$ randomly select a triplet of fresh authentication shares $\{(\langle A \rangle_b, \langle \alpha A \rangle_b), (\langle B \rangle_b, \langle \alpha B \rangle_b), (\langle C \rangle_b, \langle \alpha C \rangle_b)\}$ (see **Figure 7** for selection details), where triple $(A, B, C) \in \mathbb{F}_p^3$ satisfying $AB = C$.
- S_0 interacts with S_1 to reveal $\Gamma = \mathbf{u} - A$ and $\Lambda = g_2 - B$.
- $S_b, b \in \{0, 1\}$ computes the $\langle z_2 \rangle_b = \langle \mathbf{u} \cdot \mathbf{sign}(\mathbf{u}) \rangle_b$ through $\langle z_2 \rangle_b = \langle C \rangle_b + \Gamma \cdot \langle B \rangle_b + \Lambda \cdot \langle A \rangle_b + \Gamma \cdot \Lambda$. Also, $\langle z_3 \rangle_b = \langle \alpha \mathbf{u} \cdot \mathbf{sign}(\mathbf{u}) \rangle_b$ can be obtained by a similarly way.

Figure 5: Our protocol for the nonlinear layer $\pi_{\text{Non-lin}}^f$

our optimized HE algorithm, and non-linear operations (including ReLU and MaxPool) are encapsulated into the GC for efficient computation.

The whole inference process can be divided into two phases. (1) *Evaluation* phase: we perform the computation of alternating linear and nonlinear layers with appropriate parameters. (2) *Consistency checking* phase: after evaluation, the server verifies the consistency of the calculations so far. The output will be released to the client if the check passes. In Appendix F, we provide details of the complete inference protocol, and give a formal theoretical analysis to validate the security of the designed protocol under the malicious client threat model. In particular, we claim that SIMC 2.0 has the following security property:

Theorem 2. *Our secure inference protocol π_{inf} is secure against a semi-honest server S_0 and any malicious adversary \mathcal{A} that corrupts the client S_1 .*

Proof. Please refer to Appendix F. \square

V. PERFORMANCE EVALUATION

In this section, we conduct experiments to demonstrate the performance of SIMC 2.0. Since SIMC 2.0 is derived from SIMC [10]³, the most advanced solution for secure inference under the client-malicious model, we take it as the baseline for

comparing the computation and communication overheads. In more detail, we first describe the performance comparison of these two approaches for linear layer computation (including matrix-vector computation and convolution), and then discuss their overheads in secure computation of non-linear layers. Finally, we demonstrate the end-to-end performance advantage of SIMC 2.0 compared to SIMC for various mainstream DNN models (e.g., AlexNet, VGG-16, ResNet-18, ResNet-50, ResNet-100, and ResNet-152).

A. Implementation Details

Consistent with SIMC, SIMC 2.0 uses the homomorphic encryption library provided by SEAL [29] (the maximum number n of slots allowed for a single ciphertext is set to 4096) to realize the calculation of linear layers, and uses the components of the garbled circuit in the EMP toolkit [30] (with the OT protocol that resists active adversaries) to realize the execution of nonlinear layers. As a result, SIMC 2.0 provides 128 bits of computational security and 40 bits of statistical security. Like SIMC, our system is implemented on the 44-bit prime field. Other parameters, such as the configuration of the zero-knowledge proof protocol [21] and the random numbers used to verify the consistency of the calculation, are completely inherited from the SIMC settings (refer to [10] for more details). Our experiments are carried out in both the LAN and WAN settings. LAN is implemented with two workstations in our lab. The client workstation has AMD

³Code is available at <https://aka.ms/simc>.

EPYC 7282 1.4GHz CPUs with 32 threads on 16 cores and 32GB RAM. The server workstation has Intel(R) Xeon(R) E5-2697 v3 2.6GHz CPUs with 28 threads on 14 cores and 64GB RAM. The WAN setting is based on a connection between a local PC and an Amazon AWS server with an average bandwidth of 963Mbps and running time of around 14ms.

B. Performance of Linear Layers

We compare the cost of SIMC 2.0 and SIMC in the linear layer. As mentioned in Section II-C, given a $n_o \times n_i$ -dimensional matrix and a vector of length n_i , the matrix-vector multiplication in SIMC only produces one ciphertext, while our method derives $n_i \cdot n_o / (l \cdot n)$ ciphertexts. The smaller l is, the greater the computational advantage our scheme obtains compared to SIMC. For comparison simplicity, we set $l = n_i \cdot n_o / (n)$ to ensure that SIMC outputs only one ciphertext for matrix-vector multiplication, which makes SIMC and SIMC 2.0 have exactly the same communication overhead at the linear layer, so that we can focus on the comparison of computation cost.

TABLE II: Cost of matrix-vector multiplication

| Dimension | Metric | # operations | | Running time (ms) | | | |
|-----------------|----------|--------------|----------|-------------------|------|--------------------|-----------------|
| | | SIMC | SIMC 2.0 | SIMC | | SIMC 2.0 (Speedup) | |
| | | | | LAN | WAN | LAN | WAN |
| 1×4096 | Rotation | 12 | 0 | | | | |
| | ScMult | 1 | 1 | 14.4 | 39.9 | 1.6 | 28.5 |
| | Add | 12 | 0 | | | (8.8 \times) | (1.4 \times) |
| 2×2048 | Rotation | 11 | 0 | | | | |
| | ScMult | 1 | 1 | 13.4 | 38.7 | 3.0 | 27.6 |
| | Add | 11 | 0 | | | (4.4 \times) | (1.4 \times) |
| 4×1024 | Rotation | 10 | 0 | | | | |
| | ScMult | 1 | 1 | 13.1 | 38.8 | 2.98 | 27.7 |
| | Add | 10 | 0 | | | (4.4 \times) | (1.4 \times) |
| 8×512 | Rotation | 9 | 0 | | | | |
| | ScMult | 1 | 1 | 11.3 | 36.6 | 3.8 | 28.1 |
| | Add | 9 | 0 | | | 2.97 (\times) | (1.3 \times) |
| 16×256 | Rotation | 8 | 0 | | | | |
| | ScMult | 1 | 1 | 10.8 | 36.5 | 3.01 | 28 |
| | Add | 8 | 0 | | | (3.5 \times) | (1.3 \times) |
| 32×128 | Rotation | 7 | 0 | | | | |
| | ScMult | 1 | 1 | 10.1 | 35.7 | 3.1 | 29.1 |
| | Add | 7 | 0 | | | (3.3 \times) | (1.2 \times) |

1) *Matrix-Vector Multiplication*: TABLE II provides the computation complexity of SIMC and SIMC 2.0 for matrix-vector multiplication with different matrix dimensions. We observe that SIMC 2.0 greatly reduces the number of most expensive rotation operations (zero time) in HE while SIMC requires up to 12 operations (which can be calculated using the formulas in TABLE I). In addition, SIMC 2.0 is very friendly to other homomorphic operations, including addition and multiplication. For example, the execution process involves only 1 multiplication compared to SIMC. The running time is also provided in TABLE II, which quantifies the entire time cost for one inference session, including client processing, server processing and network latency. We observe that in the LAN setting, SIMC 2.0 can achieve the speedup by up to 8.8 \times for matrix-vector multiplication of different dimensions. This is mainly due to our optimization strategy for this operation. Specifically, we first divide the server's original $n_o \times n_i$ -dimensional weight matrix into multiple submatrices and calculate each submatrix separately. It can effectively reduce the number of rotations required for the

client's ciphertext from $n_o - 1$ to $l - 1$. Then we convert the subsequent rotation operations by summing in the ciphertext into the plaintext (see Section II-C), thereby removing all the homomorphic rotation operations required at this stage.

We observe that the speedup of SIMC 2.0 is relatively smaller under the WAN setting, which is mainly caused by the communication latency between the local client and the cloud server. This dominates the total running time compared to the computation cost of the lightweight HE. Particularly, the running time is round 14 milliseconds in our setting, while the optimized HE in SIMC 2.0 only takes about 1 to 3 milliseconds.

2) *Convolution Computation*: The complexity and running time of the convolution operation for different input sizes and kernel sizes are provided in TABLE III, where the encrypted input is a data sample of size $u_w \times u_h$ with c_i channels (denoted as $u_w \times u_h @ c_i$) and the server holds kernels with the size of $k_w \times k_h @ c_o$ and c_i channels per kernel. We observe that our method substantially reduces the number of rotation operations required to compute the convolution compared to SIMC. For example, SIMC 2.0 reduces the number of rotation operations by up to 127 \times compared to SIMC, given the input size of $16 \times 16 @ 2048$ and kernel size of $1 \times 1 @ 512$. This benefits from our designed kernel grouping method, which reduces the most expensive rotation operation by a factor of $\frac{c_i}{c_n}$ (refer to Appendix D for more details). The results indicate that a large speedup can be obtained if the input has more channels and a small kernel size. This is very beneficial for modern models which commonly have such characteristics. For the running time, it is obvious that our method significantly accelerates the inference execution. In more detail, in the LAN setting, SIMC 2.0 achieves speedups of 5.7 \times , 17.4 \times , 2.5 \times , and 1.7 \times compared to SIMC. In the WAN setting, SIMC 2.0 also shows similar performance superiority.

TABLE III: Cost of convolution computation

| Input | Kernel | Metric | #operations | | Running time (s) | | | |
|-----------------------|--------------------|----------|-------------|--------|------------------|------|--------------------|------------------|
| | | | SIMC | Ours | SIMC | | SIMC 2.0 (Speedup) | |
| | | | | | LAN | WAN | LAN | WAN |
| $16 \times 16 @ 128$ | $1 \times 1 @ 128$ | Rotation | 960 | 120 | | | | |
| | | ScMult | 1024 | 1024 | 1.3 | 1.4 | 0.23 | 0.35 |
| | | Add | 1016 | 1016 | | | (5.7 \times) | (4.0 \times) |
| $16 \times 16 @ 2048$ | $1 \times 1 @ 512$ | Rotation | 61140 | 480 | | | | |
| | | ScMult | 65536 | 65536 | 79.9 | 81.0 | 4.60 | 5.13 |
| | | Add | 65504 | 65504 | | | (17.4 \times) | (15.8 \times) |
| $16 \times 16 @ 128$ | $3 \times 3 @ 128$ | Rotation | 1024 | 184 | | | | |
| | | ScMult | 9216 | 9216 | 2.6 | 2.8 | 1.04 | 1.22 |
| | | Add | 9208 | 9208 | | | (2.5 \times) | (2.3 \times) |
| $16 \times 16 @ 2048$ | $5 \times 5 @ 64$ | Rotation | 10752 | 3132 | | | | |
| | | ScMult | 204800 | 204800 | 41.3 | 42.0 | 24.3 | 26.3 |
| | | Add | 204796 | 204796 | | | (1.7 \times) | (1.6 \times) |

C. Performance of Non-linear Layers

We compare the computation and communication overheads of SIMC and our SIMC 2.0 in the implementation of non-linear layers. We mainly show the cost required by the two schemes to securely execute different numbers of ReLU functions.

1) *Computation Overhead*: FIGURES 6(a) and 6(b) show the running time of SIMC and SIMC 2.0 for different numbers

of ReLU functions under the LAN and WAN settings, respectively. We observe that SIMC 2.0 reduces the running time by about one-third compared to SIMC. Our improvement mainly comes from the optimization mechanism designed for the computation of non-linear layers. As mentioned earlier, compared to SIMC, we only encapsulate the non-linear part of ReLU into the GC. The goal of this strategy is to substantially reduce the number of AND gates required in the GC (AND operations are usually expensive in the GC). For example, given GC’s security parameter $\lambda = 128$ bits and 44-bit prime field, SIMC needs 249 AND gates to calculate ReLU while we only need 161 AND gates. This saves 88 AND gate operations! Moreover, the alternative protocol we designed is also resource-friendly, requiring only the server and client to exchange two elements and perform simple mathematical operations locally.

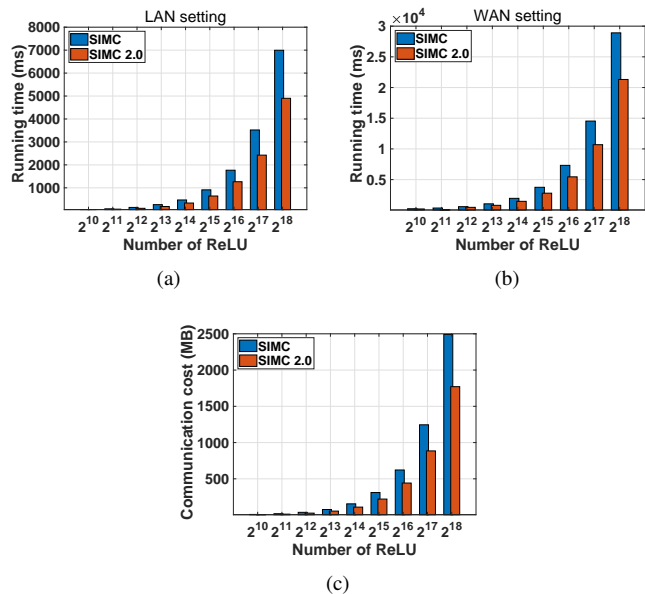


Fig. 6: Comparison of the nonlinear layer overhead. (a) Running time under the LAN setting. (b) Running time under the WAN setting. (c) Communication overhead with different numbers of ReLU functions.

2) *Communication Overhead*: **Figure 6(c)** provides the communication overhead incurred by SIMC and our method in computing different numbers of ReLU functions. We observe that SIMC 2.0 reduces the communication overhead of SIMC by approximately one-third. This also benefits from our optimized GC to perform non-linear operations. In more detail, given GC’s security parameter $\lambda = 128$ bits and 44-bit prime field, SIMC requires to communicate 11.92 KB data to perform one ReLU. In contrast, since our optimized GC saves about 88 AND gates, which needs 2.69 KB communication data for each ReLU, our SIMC 2.0 only requires 9.21 KB data transfer for each ReLU. Note that such communication advantages are non-trivial since mainstream DNN models usually contain tens of thousands of ReLU functions.

D. Performance of End-to-end Secure Inference

Finally we compare the computation and communication costs of SIMC and SIMC 2.0 for different complete DNN models. We employ 7 ML models in our experiments: (1) a multi-layer perceptron with the network structure of 784-128-128-10, which is often used for benchmarking private-preserving model deployment (*e.g.*, SecureML [5], MiniONN [31], GAZELLE). This model is trained with the MNIST dataset. (2) Some mainstream CNN models: AlexNet[32], VGG-16 [33], ResNet-18 [34], ResNet-50 [34], ResNet-101 [34], and ResNet-152 [34]. These models are trained over the CIFAR-10 dataset.

TABLE IV: Cost of end-to-end model inference

| Model | Metric | #operations | | Running time (s) | | | | Comm. (GB) | |
|------------|----------|-------------|-----------------|------------------|--------|------------------------|------------------------|------------|-------|
| | | SIMC | Ours | SIMC | | SIMC 2.0 (Speedup) | | SIMC | Ours |
| | | | | LAN | WAN | LAN | WAN | | |
| MLP | Rotation | 70 | 55 | 0.14 | 0.21 | 0.11 (1.3×) | 0.18 (1.2×) | ;0.01 | ;0.01 |
| | ScMult | 56 | 56 | | | | | | |
| | Add | 70 | 55 | | | | | | |
| AlexNet | Rotation | 72549 | 4394 | 81.0 | 85.8 | 35.2 (2.3×) | 47.7 (1.8×) | 0.42 | 0.29 |
| | ScMult | 931977 | 931977 | | | | | | |
| | Add | 931643 | 931630 | | | | | | |
| VGG-16 | Rotation | 315030 | 10689 | 72.4 | 97.6 | 34.5 (2.1×) | 54.2 (1.8×) | 5.81 | 4.13 |
| | ScMult | 3677802 | 3677802 | | | | | | |
| | Add | 3676668 | 3676654 | | | | | | |
| ResNet-18 | Rotation | 234802 | 9542 | 77.1 | 118.3 | 35.0 (2.2×) | 65.6 (1.8×) | 4.27 | 3.04 |
| | ScMult | 2737585 | 2737585 | | | | | | |
| | Add | 2736632 | 2736624 | | | | | | |
| ResNet-50 | Rotation | 2023606 | 50666 | 434.8 | 683.9 | 111.3 (3.9×) | 296.4 (2.3×) | 29.50 | 21.00 |
| | ScMult | 5168181 | 5168181 | | | | | | |
| | Add | 5162524 | 5162518 | | | | | | |
| ResNet-101 | Rotation | 3947190 | 113770 | 802.3 | 1195.2 | 186.5 (4.3×) | 478.1 (2.5×) | 46.13 | 31.85 |
| | ScMult | 9903157 | 9903157 | | | | | | |
| | Add | 9890972 | 9890964 | | | | | | |
| ResNet-152 | Rotation | 5533878 | 169450 | 1209.2 | 1780.1 | 274.8 (4.4×) | 684.6 (2.6×) | 64.25 | 46.28 |
| | ScMult | 13802549 | 13802549 | | | | | | |
| | Add | 13784604 | 13784596 | | | | | | |

TABLE IV provides the computation complexity of SIMC and our method for different models. It is clear that SIMC 2.0 reduces the number of rotation operations in SIMC by 16.5×, 29.4×, 24.6×, 39.9×, 34.6× and 50.5× for AlexNet, VGG-16, ResNet-18, ResNet-50, ResNet-101, and ResNet-152, respectively. The fundamental reason for this improvement is that our designed optimization technique is for HE-based linear operations. We observe that SIMC 2.0 does not significantly reduce the number of rotation operations in the MLP model. It stems from the small ratio between the number of slots and the dimension of the output in the MLP, which limits the performance gain. **TABLE IV** also shows the running time and the corresponding speedup of our scheme. Since we substantially reduce the number of expensive rotation operations in the linear layer, and design an optimized GC for the nonlinear layer, our method obtains speedups of 2.3×, 2.1×, 2.2×, 3.9×, 4.3× and 4.4× for AlexNet, VGG-16, ResNet-18, ResNet-50, ResNet-101, and ResNet-152, respectively, under the LAN Setting. A similar performance boost is obtained under the WAN setting. Due to network latency in the WAN, the running time of both SIMC and our method is inevitably increased. This can reduce the performance advantage of SIMC 2.0, but our solution is still better than SIMC.

It has been demonstrated that for the HE-GC based secure inference model, the communication overhead caused by the non-linear layer dominates the communication in SIMC (refer to Section 5 in SIMC [10]). In our experiments, the

communication cost of linear layers in SIMC 2.0 remains consistent with SIMC, while the overhead of nonlinear layers is reduced by two-thirds. Therefore, we observe that the size of communication data required by SIMC 2.0 is still smaller than SIMC, remaining approximately between $2/3 \sim 3/4$ of the original size, depending on the model size. For example, for the ResNet-152 model, SIMC requires to transfer 64.25 GB data to perform an inference process while our SIMC 2.0 saves about 18GB in the communication overhead, which is quite impressive.

VI. CONCLUSION

In this paper, we proposed SIMC 2.0, which significantly improves the performance of SIMC for secure ML inference in a threat model with a malicious client and honest-but-curious server. We designed a new coding method to minimize the number of costly rotation operations during homomorphic parallel matrix and vector computations in the linear layers. We also greatly reduced the size of the GC in SIMC to substantially speed up operations in the non-linear layers. In the future, we will focus on designing more efficient optimization strategies to further reduce the computation overhead of SIMC 2.0, to make secure ML inference more suitable for a wider range of practical applications.

REFERENCES

- [1] J. Katz, S. Ranellucci, and et al, "Optimizing authenticated garbling for faster secure two-party computation," in *Annual International Cryptology Conference (CRYPTO)*. Springer, 2018, pp. 365–391.
- [2] X. Wang, A. J. Malozemoff, and J. Katz, "Faster secure two-party computation in the single-execution setting," in *Annual International Conference on the Theory and Applications of Cryptographic Techniques (EUROCRYPT)*. Springer, 2017, pp. 399–424.
- [3] D. Rathee, M. Rathee, and et al, "Cryptflow2: Practical 2-party secure inference," in *Proceedings of the ACM SIGSAC Conference on Computer and Communications Security (CCS)*, 2020, pp. 325–342.
- [4] A. Patra, T. Schneider, and et al, "Aby2. 0: Improved mixed-protocol secure two-party computation," in *USENIX Security Symposium*, 2021.
- [5] P. Mohassel and Y. Zhang, "Secureml: A system for scalable privacy-preserving machine learning," in *2017 IEEE symposium on security and privacy (S&P)*. IEEE, 2017, pp. 19–38.
- [6] R. LaVigne, C.-D. Liu-Zhang, and et al, "Topology-hiding computation beyond semi-honest adversaries," in *Theory of Cryptography Conference (TCC)*. Springer, 2018, pp. 3–35.
- [7] S. U. Hussain, M. Javaheripi, and et al, "Coinn: Crypto/ml codesign for oblivious inference via neural networks," in *Proceedings of the ACM SIGSAC Conference on Computer and Communications Security (CCS)*, 2021, pp. 3266–3281.
- [8] Q. Lou and L. Jiang, "Hemet: A homomorphic-encryption-friendly privacy-preserving mobile neural network architecture," in *International Conference on Machine Learning (ICML)*. PMLR, 2021, pp. 7102–7110.
- [9] R. Lehmkuhl, P. Mishra, and et al, "Muse: Secure inference resilient to malicious clients," in *USENIX Security Symposium*, 2021.
- [10] N. Chandran, D. Gupta, and et al, "Simc: ML inference secure against malicious clients at semi-honest cost," in *USENIX Security Symposium*, 2022.
- [11] A. Patra and A. Suresh, "Blaze: Blazing fast privacy-preserving machine learning," in *Proceedings of the Network and Distributed System Security (NDSS)*, 2020.
- [12] I. Damgård, D. Escudero, and et al, "New primitives for actively-secure mpc over rings with applications to private machine learning," in *IEEE Symposium on Security and Privacy (S&P)*. IEEE, 2019, pp. 1102–1120.
- [13] D. Escudero, S. Ghosh, and et al, "Improved primitives for mpc over mixed arithmetic-binary circuits," in *Annual International Cryptology Conference (CRYPTO)*. Springer, 2020, pp. 823–852.
- [14] C. Hazay and A. Yanai, "Constant-round maliciously secure two-party computation in the ram model," *Journal of Cryptology*, vol. 32, no. 4, pp. 1144–1199, 2019.
- [15] P. Mishra, R. Lehmkuhl, and et al, "Delphi: A cryptographic inference service for neural networks," in *USENIX Security Symposium*, 2020, pp. 2505–2522.
- [16] Q. Zhang, C. Xin, and H. Wu, "Gala: Greedy computation for linear algebra in privacy-preserved neural networks," in *Proceedings of the Network and Distributed System Security (NDSS)*, 2021.
- [17] S. Sav, A. Pyrgelis, and et al, "Poseidon: Privacy-preserving federated neural network learning," in *Proceedings of the Network and Distributed System Security (NDSS)*, 2021.
- [18] Z. Huang, W.-j. Lu, C. Hong, and J. Ding, "Cheetah: Lean and fast secure two-party deep neural network inference," *Cryptology ePrint Archive*, 2022.
- [19] X. Jiang, M. Kim, and et al, "Secure outsourced matrix computation and application to neural networks," in *Proceedings of the ACM SIGSAC Conference on Computer and Communications Security (CCS)*, 2018, pp. 1209–1222.
- [20] C. Juvekar, V. Vaikuntanathan, and et al, "{GAZELLE}: A low latency framework for secure neural network inference," in *USENIX Security Symposium*, 2018, pp. 1651–1669.
- [21] H. Chen, M. Kim, and et al, "Maliciously secure matrix multiplication with applications to private deep learning," in *International Conference on the Theory and Application of Cryptology and Information Security (ASIACRYPT)*. Springer, 2020, pp. 31–59.
- [22] N. Chandran, D. Gupta, and et al, "Ezpc: programmable and efficient secure two-party computation for machine learning," in *IEEE European Symposium on Security and Privacy (EuroS&P)*. IEEE, 2019, pp. 496–511.
- [23] D. Demmler, T. Schneider, and M. Zohner, "Aby-a framework for efficient mixed-protocol secure two-party computation," in *Proceedings of the Network and Distributed System Security (NDSS)*, 2015.
- [24] X. Wang, S. Ranellucci, and J. Katz, "Authenticated garbling and efficient maliciously secure two-party computation," in *Proceedings of the ACM SIGSAC Conference on Computer and Communications Security (CCS)*, 2017, pp. 21–37.
- [25] S. Halevi and V. Shoup, "Algorithms in helib," in *Annual Cryptology Conference (CRYPTO)*. Springer, 2014, pp. 554–571.
- [26] M. Keller, E. Orsini, and P. Scholl, "Actively secure ot extension with optimal overhead," in *Annual Cryptology Conference (CRYPTO)*. Springer, 2015, pp. 724–741.
- [27] Z. Ghodsi, N. K. Jha, B. Reagen, and S. Garg, "Circa: Stochastic relus for private deep learning," *Advances in Neural Information Processing Systems (NeurIPS)*, vol. 34, 2021.
- [28] S. Zahir, M. Rosulek, and D. Evans, "Two halves make a whole," in *Annual International Conference on the Theory and Applications of Cryptographic Techniques (EUROCRYPT)*. Springer, 2015, pp. 220–250.
- [29] "Microsoft SEAL (release 3.3)," <https://github.com/Microsoft/SEAL>, Jun. 2019, microsoft Research, Redmond, WA.
- [30] X. Wang, A. J. Malozemoff, and J. Katz, "Emp-toolkit: Efficient multiparty computation toolkit," <https://github.com/emp-toolkit>, 2016.
- [31] J. Liu, M. Juuti, Y. Lu, and N. Asokan, "Oblivious neural network predictions via minion transformations," in *Proceedings of the 2017 ACM SIGSAC conference on computer and communications security (CCS)*, 2017, pp. 619–631.
- [32] W. Yu, K. Yang, and et al, "Visualizing and comparing alexnet and vgg using deconvolutional layers," in *Proceedings of the International Conference on Machine Learning (ICML)*, 2016.
- [33] K. Simonyan and A. Zisserman, "Very deep convolutional networks for large-scale image recognition," in *Proceedings of the International Conference on Learning Representations (ICLR)*, 2015.
- [34] K. He, X. Zhang, S. Ren, and J. Sun, "Deep residual learning for image recognition," in *Proceedings of the IEEE conference on computer vision and pattern recognition (CVPR)*, 2016, pp. 770–778.
- [35] Y. Lindell, "How to simulate it—a tutorial on the simulation proof technique," *Tutorials on the Foundations of Cryptography*, pp. 277–346, 2017.
- [36] M. Keller, V. Pastro, and D. Rotaru, "Overdrive: Making spdz great again," in *Annual International Conference on the Theory and Applications of Cryptographic Techniques (EUROCRYPT)*. Springer, 2018, pp. 158–189.

Input: S_1 holds $(\langle A \rangle_1, \langle B \rangle_1)$ uniformly chosen from \mathbb{F}_p . S_0 holds $(\langle A \rangle_0, \langle B \rangle_0)$ and a MAC key α uniformly chosen from \mathbb{F}_p .

Output: S_b obtains $\{(\langle A \rangle_b, \langle \alpha A \rangle_b), (\langle B \rangle_b, \langle \alpha B \rangle_b), (\langle C \rangle_b, \langle \alpha C \rangle_b)\}$ for $b \in \{0, 1\}$.

Procedure:

- S_0 and S_1 participate in a two-party secure computing protocol against the semi-honest server S_0 and the malicious client S_1 , so that S_1 obtains an FHE's public and secret key (pk, sk) and S_0 obtains pk . This process is performed only once.
- S_1 send the encryptions $c_1 \leftarrow \text{Enc}(pk, A_1)$ and $c_2 \leftarrow \text{Enc}(pk, B_1)$ to S_0 along with a zero-knowledge (ZK) proof of plaintext knowledge of the two ciphertexts. A ZK proof of knowledge for ciphertexts is used to state that c_1 and c_2 are valid ciphertexts generated from the given FHE cryptosystem. Readers can refer to [36], [21] for more details.
- S_0 samples $(\langle \alpha A \rangle_0, \langle \alpha B \rangle_0, \langle \alpha C \rangle_0, \langle C \rangle_0)$ from \mathbb{F}_p^3 , and then computes $c_3 = \text{Enc}_{pk}(\alpha(\langle A \rangle_0 + \langle A \rangle_1) - \langle \alpha A \rangle_0)$, $c_4 = \text{Enc}_{pk}(\alpha(\langle B \rangle_0 + \langle B \rangle_1) - \langle \alpha B \rangle_0)$, $c_5 = \text{Enc}_{pk}(\alpha(A \cdot B) - \langle \alpha C \rangle_0)$, and $c_6 = \text{Enc}_{pk}((A \cdot B) - \langle C \rangle_0)$.
- S_1 decrypts c_3, c_4, c_5 and c_6 to obtain $(\langle \alpha A \rangle_1, \langle \alpha B \rangle_1, \langle \alpha C \rangle_1, \langle C \rangle_1)$.
- S_b outputs $\{(\langle A \rangle_b, \langle \alpha A \rangle_b), (\langle B \rangle_b, \langle \alpha B \rangle_b), (\langle C \rangle_b, \langle \alpha C \rangle_b)\}$ for $b \in \{0, 1\}$.

Figure 7: Algorithm of generating authenticated Beaver's multiplicative triple

Input: S_0 holds $\mathbf{N} \in \mathbb{F}_p^{n_o \times n_i}$ and a MAC key α uniformly chosen from \mathbb{F}_p . S_1 holds $\mathbf{t} \in \mathbb{F}_p^{n_i}$.

Output: S_b obtains $\{(\langle \mathbf{Nt} \rangle_b, \langle \alpha \mathbf{Nt} \rangle_b)\}$ for $b \in \{0, 1\}$.

Procedure:

- S_0 and S_1 participate in a two-party secure computing protocol against the semi-honest server S_0 and the malicious client S_1 , so that S_1 obtains the FHE's public and secret key (pk, sk) and S_0 obtains pk . This process is performed only once.
- S_1 sends the encryption $\mathbf{c}_1 \leftarrow \text{Enc}(pk, \mathbf{t})$ to S_0 along with a zero-knowledge (ZK) proof of plaintext knowledge of this ciphertext.
- S_0 samples $(\langle \mathbf{Nt} \rangle_0, \langle \alpha \mathbf{Nt} \rangle_0)$ from $\mathbb{F}_p^{n_o}$, and then sends $\mathbf{c}_2 = \text{Enc}_{pk}(\mathbf{Nt} - \langle \mathbf{Nt} \rangle_0)$ and $\mathbf{c}_3 = \text{Enc}_{pk}(\alpha \mathbf{Nt} - \langle \alpha \mathbf{Nt} \rangle_0)$ to S_1 .
- S_1 decrypts \mathbf{c}_2 and \mathbf{c}_3 and set $\langle \mathbf{Nt} \rangle_1 = \text{Dec}_{sk}(\mathbf{c}_2)$, $\langle \alpha \mathbf{Nt} \rangle_1 = \text{Dec}_{sk}(\mathbf{c}_3)$.
- S_b outputs $\{(\langle \mathbf{Nt} \rangle_b, \langle \alpha \mathbf{Nt} \rangle_b)\}$ for $b \in \{0, 1\}$.

Figure 8: Protocol of **InitLin**

APPENDIX APPENDIX A THREAT MODEL

We present the formal security using the simulation paradigm [35]. Security is modeled through two interactive protocols: a real interactive protocol where S_0 and S_1 execute the protocol in the presence of an adversary \mathbf{A} and an environment Z , and an ideal interactive protocol where the parties send input to a trusted third party who performs the computation faithfully. Security requires that for any adversary \mathbf{A} , there is a simulator \mathbf{S} in the ideal interaction, which enables no environment Z to distinguish between the ideal and the real interactions. Specifically, Let $f = (f_0, f_1)$ be the functionality of the two parties so that S_0 learns $f_0(x, y)$

and S_1 learns $f_1(x, y)$ with x and y as inputs, respectively. Hence, we say that a protocol π securely implements f on the *client-malicious* adversary model if the following properties are held.

- **Correctness:** If S_0 and S_1 are both honest, then S_0 gets $f_0(x, y)$ and S_1 gets $f_1(x, y)$ from the execution of π on the inputs x and y , respectively.
- **Semi-honest Server Security:** For the semi-honest adversary S_0 , there exists a simulator \mathbf{S} , so that for any input (x, y) , we have

$$\text{View}_{\mathbf{A}}^{\pi}(x, y) \approx \mathbf{S}(x, f_0(x, y))$$

where $\text{View}_{\mathbf{A}}^{\pi}(x, y)$ denotes \mathbf{A} 's view during the execution of π given the S_0 's input x and S_1 's input y . $\mathbf{S}(x, f_0(x, y))$ represents the view simulated by \mathbf{S} when it is given access to x and $f_0(x, y)$ of S_0 . \approx indicates computational indistinguishability of two distributions $\text{View}_{\mathbf{A}}^{\pi}(x, y)$ and $\mathbf{S}(x, f_0(x, y))$.

- **Malicious Client Security:** For the malicious adversary S_1 , there exists a simulator \mathbf{S} , so that for any input x from S_0 , we have

$$\text{Out}_{S_0}, \text{View}_{\mathbf{A}}^{\pi}(x, \cdot) \approx \hat{\text{Out}}, \mathbf{S}^{f(x, \cdot)}$$

where $\text{View}_{\mathbf{A}}^{\pi}(x, \cdot)$ denotes \mathbf{A} 's view during the execution of π given the S_0 's input x . Out_{S_0} indicates the output of S_0 in the same protocol execution. Similarly, $\hat{\text{Out}}$ and $\mathbf{S}^{f(x, \cdot)}$ represents the output of S_0 and the view simulated by \mathbf{S} in an ideal interaction.

APPENDIX B GENERATION OF AUTHENTICATED BEAVER'S MULTIPLICATIVE TRIPLE

APPENDIX C PROTOCOLS OF INITLIN AND LIN

APPENDIX D OPTIMIZATION FOR CONVOLUTION OPERATIONS

We show how to compute convolutional layers in a parallelized manner, where we mainly incorporate the core idea of work GALA [16]. We reuse the symbols \mathbf{N} and $[\mathbf{t}]_c$ used in

Input: S_0 holds $\mathbf{N} \in \mathbb{F}_p^{n_o \times n_i}$, a MAC key α uniformly chosen from \mathbb{F}_p , and $\langle \mathbf{t} \rangle_0, \langle \mathbf{d} \rangle_0 \in \mathbb{F}_p^{n_i}$. S_1 holds $\langle \mathbf{t} \rangle_1, \langle \mathbf{d} \rangle_1 \in \mathbb{F}_p^{n_i}$, where $\mathbf{d} = \alpha \mathbf{t}$.

Output: S_b obtains $\{(\langle \mathbf{Nt} \rangle_b, \langle \mathbf{Nd} \rangle_b, \langle \alpha^3 \mathbf{t} - \alpha^2 \mathbf{d} \rangle_b)\}$ for $b \in \{0, 1\}$.

Procedure:

- S_1 sends the encryptions $\mathbf{e}_1 \leftarrow \text{Enc}(pk, \langle \mathbf{t} \rangle_1)$ and $\mathbf{e}_2 \leftarrow \text{Enc}(pk, \langle \mathbf{d} \rangle_1)$ to S_0 along with a zero-knowledge (ZK) proof of plaintext knowledge of the two ciphertexts.
- S_0 samples $(\langle \mathbf{Nt} \rangle_0, \langle \mathbf{Nd} \rangle_0)$ from $\mathbb{F}_p^{n_o}$ and $\langle \alpha^3 \mathbf{t} - \alpha^2 \mathbf{d} \rangle_0$ from $\mathbb{F}_p^{n_i}$.
- S_0 computes $\mathbf{e}_3 = \text{Enc}_{pk}(\mathbf{Nt} - \langle \mathbf{Nt} \rangle_0)$, $\mathbf{e}_4 = \text{Enc}_{pk}(\mathbf{Nd} - \langle \mathbf{Nd} \rangle_0)$, and $\mathbf{e}_5 = \alpha^3 \mathbf{t} - \alpha^2 \mathbf{d} - \langle \alpha^3 \mathbf{t} - \alpha^2 \mathbf{d} \rangle_0$. S_0 sends $\mathbf{e}_3, \mathbf{e}_4$ and \mathbf{e}_5 to S_1 .
- S_1 sets $\langle \mathbf{Nt} \rangle_1 = \text{Dec}_{sk}(\mathbf{e}_3)$, $\langle \mathbf{Nd} \rangle_1 = \text{Dec}_{sk}(\mathbf{e}_4)$, and $\langle \alpha^3 \mathbf{t} - \alpha^2 \mathbf{d} \rangle_1 = \text{Dec}_{sk}(\mathbf{e}_5)$.
- S_b outputs $\{(\langle \mathbf{Nt} \rangle_b, \langle \mathbf{Nd} \rangle_b, \langle \alpha^3 \mathbf{t} - \alpha^2 \mathbf{d} \rangle_b)\}$ for $b \in \{0, 1\}$.

Figure 9: Protocol of **Lin**

computing the matrix-vector multiplication, which represent the inputs held by the server and client, respectively. To be precise, we assume that the server has c_o plaintext kernels of size $k_w \times k_h \times c_i$, and the ciphertext input sent by the client to the server is c_i kernels of size $u_w \times u_h$. The server is required to perform homomorphic convolution operations between the ciphertext input and its own plaintext kernel to obtain the ciphertext output. We first describe the basic convolution operation under single-input single-output (SISO), and then we extend this to the general case of multiple-input multiple-output (MIMO) (the method designed in GAZELLE [20]). Finally, we show the details of our method which exhibits better computational performance.

A. Basic Convolution for the Single Input Single Output (SISO)

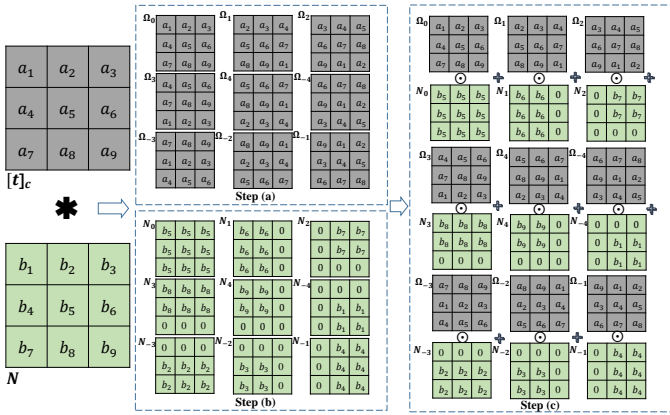


Fig. 10: SISO convolution

SISO is a special case of MIMO where $c_i = c_o = 1$. Therefore, the client's encrypted input is a data (*i.e.*, a 2D image) of size $u_w \times u_h$ with one channel and the server holds a 2D filter of size $k_w \times k_h$ with one kernel. **Figure 10** gives an example where $[t]_c$ is the input from the client and N represents the plaintext kernel held by the server. The convolution computation process can be visualized as first placing N at different positions of the $[t]_c$. Then, for each location, the sum of the element-wise products of the kernel and the corresponding data value within the kernel window is computed. As shown in **Figure 10**, the first value of the convolution between $[t]_c$ and N is $(a_1b_5 + a_2b_6 + a_4b_8 + a_5b_9)$. It is obtained by first placing the center of N , *i.e.* b_5 at the position of a_1 , and then computing the element-wise product between N and the part of $[t]_c$ that is within N 's kernel window (*i.e.*, a_1, a_2, a_4 and a_5). Similarly, the remaining convolution results can be computed sequentially by placing b_5 in a_2 to a_9 .

We take **Figure 10** as an example to illustrate the basic SISO procedure in detail, where b_5 is first placed in the position of a_5 . We observe that the kernel size is $k_w \times k_h = 9$. The final convolution result is obtained by summing the element-wise products between the 9 values in N and the corresponding 9 values around a_5 . This can be done by rotating $[t]_c$ in a raster scan manner. Specifically, we first convert $[t]_c$ to the equivalent

vector format and perform $(k_w \times k_h - 1)$ round rotations on it, with the first half forward and the remaining half in the backward direction. We use the notation Ω_j to indicate that $[t]_c$ is rotated by j positions, where a positive j represents the forward direction and a negative j represents the backward direction (as shown in Step(a) in **Figure 10**).

When given all Ω_j , the coefficients of the plaintext kernel N also need to be re-encoded accordingly (See N_j in step(b) in **Figure 10**) based on the procedure of convolution operation. Then, each Ω_j performs an element-wise product with the corresponding N_j and we get the final encrypted results by summing up all the ciphertexts (shown in step(c) in **Figure 10**). As for the computation complexity, SISO requires a total of $(k_w k_h - 1)$ rotation operations (excluding the trivial rotation by zero), all of which are operated on $[t]_c$, and $(k_w k_h)$ times ScMult operations and $(k_w k_h - 1)$ times Add operations.

B. MIMO Convolution (GAZELLE)

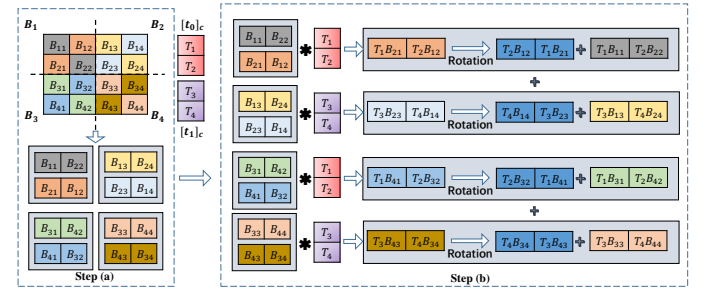


Fig. 11: MIMO convolution

We now consider the general case, *i.e.*, MIMO, where c_i or c_o is not one. A simple way is to use the above convolution operation for SISO multiple times. Specifically, the client first encrypts c_i input channels into c_i ciphertexts, $\{[t]_c\}$ and sends them to the server. Since each of c_o channels contains c_i filters, each $[t]_c$ is convolved with one of the c_i filters by way of SISO. As a result, the final ciphertext result will be obtained by summing all of the c_i SISO convolutions. Obviously, this naive approach requires $c_i(k_w k_h - 1)$ rotation operations for c_i input channels, $c_i(k_w k_h)$ ScMult operations, and $c_o(c_i k_w k_h - 1)$ addition operations. This method outputs c_o ciphertexts.

GAZELLE presents a new MIMO convolution method that substantially reduces the computation complexity compared to the naive method. Its key insight is the efficient utilization of the ciphertext slot n , due to the observation that n is usually much larger than the channel size $u_w u_h$. Specifically, to improve utilization and parallel processing capabilities, GAZELLE proposes to pack the input data of c_n channels into one ciphertext, that is, the input is now $\frac{c_i}{c_n}$ ciphertexts instead of c_i ciphertexts (see **Figure 11** where the four input channels are organized into two ciphertexts, each of which contains 2 channels). As a result, the c_o kernels held by the server can be viewed as a $c_o \times c_i$ size kernel block, where each row of the block contains c_i 2D filters for each kernel. Since then, the convolution operation of MIMO can be analogized to matrix-vector multiplication, where element-wise multiplication is replaced by convolution. Since each ciphertext contains c_n

channels, the entire kernel block can be further divided into $\frac{c_0 c_i}{c_n^2}$ blocks (as shown in Step(a) in **Figure 11**, where the kernel block is split into \mathbf{B}_1 to \mathbf{B}_4).

Each divided block will be further encoded as vectors in a diagonal manner (see Step(a) in **Figure 11**, where we rearrange the positions of elements in each divided block \mathbf{B}_i). Afterwards, we can execute convolution operations between each input ciphertext and vectors in each divided block with the SISO manner. The c_n convolved vectors will be rotated diagonally to coincide with the elements in the corresponding kernel block, thereby obtaining the convolution of each divided block with the corresponding vector. Finally, we obtain the ciphertext result by summing up all results ciphertexts(see Step(b) in **Figure 11**).

We now analyze the computation complexity introduced by GAZELLE. We observe that for each of the $\frac{c_0 c_i}{c_n^2}$ blocks, there are a total of $(c_n - 1)$ rotation operations. This requires $c_n k_w k_h$ ScMult operations and $(c_n k_w k_h - 1)$ Add operations. Additionally, there are a total of $\frac{c_i}{c_n}$ block convolutions associated with the same kernel order. Since for each of the $\frac{c_i}{c_n}$ blocks, we use the SISO method to calculate the convolution between the corresponding kernel blocks, which requires a total of $\frac{c_i (k_w k_h - 1)}{c_n}$ rotation operations. In general, MIMO convolution requires a total of $\frac{c_0 c_i}{c_n^2} (c_n - 1) + \frac{c_i (k_w k_h - 1)}{c_n}$ rotations, $k_w k_h \frac{c_i c_0}{c_n}$ ScMult and $\frac{c_0}{c_n} (c_i k_w k_h - 1)$ Add operations. This method outputs $\frac{c_0}{c_n}$ ciphertexts.

C. Our MIMO Convolution

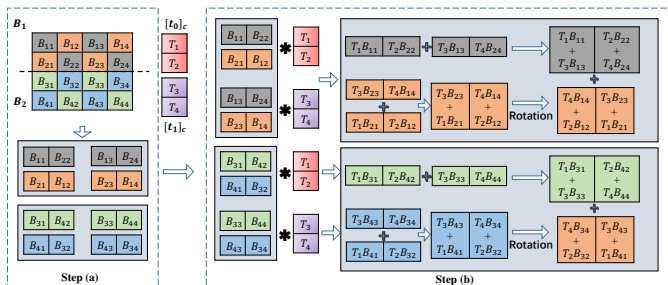


Fig. 12: Our MIMO convolution

We present an improved solution to execute the MIMO convolution based on the GAZELLE's method. Our key trick is to design strategies to significantly reduce the number of rotation operations involved in computing the convolution between each of the $\frac{c_0 c_i}{c_n^2}$ blocks and the corresponding input channels. To be precise, we find that for each of the $\frac{c_0 c_i}{c_n^2}$ blocks, GAZELLE's method requires $(c_n - 1)$ rotation operations to obtain the convolution for that block. However, since our goal is to obtain the convolution of each kernel, we actually do not need to get the convolution of each block. We propose a *first-Add-second-Rotation method* to reduce the complexity of rotations. Specifically, as shown in **Figure 12**, the entire kernel block is divided into two blocks, *i.e.*, \mathbf{B}_1 and \mathbf{B}_2 , where each block is the combination of $\frac{c_i}{c_n} c_n$ -by- c_n divided blocks, which corresponding to the same kernels (The first two kernels are contained in block \mathbf{B}_1 , while the third and fourth kernel are organized in \mathbf{B}_1).

For each newly constructed block, all its row vectors are first convolved with the corresponding input ciphertexts in a SISO manner. Then, those convolved vectors associated with the same kernel order will be added together (see add operation of Step (b) in **Figure 12** before executing rotations). Finally, these added vectors are rotated to the same kernel order and summed to obtain the final convolution result. Our method incurs $(c_n - 1)$ rotations for each of $\frac{c_0}{c_n}$ newly constructed blocks, which reduces the computation complexity with respect to rotation by a factor of $\frac{c_i}{c_n}$ compared to the method proposed by GAZELLE. This is substantially because in state-of-the-art DNN networks such as ResNets, $\frac{c_i}{c_n}$ can reach 256. This is mainly due to the fact that neural networks contain a large number of large-sized feature maps in order to capture complex input features.

We now analyze the computation complexity of our proposed method. Specifically, for each of the $\frac{c_0}{c_n}$ blocks, there are a total of c_i SISO convolutions. Additionally, there are $\frac{c_i}{c_n}$ convolutions summed for each of the c_n kernel orders, which introduces c_n added convolutions. These added convolutions will be further rotated to the same kernels and then summed up to obtain the final ciphertext result. Therefore, our method requires a total of $\frac{c_0}{c_n} (c_n - 1) + \frac{c_i (k_w k_h - 1)}{c_n}$ rotations, $k_w k_h \frac{c_i c_0}{c_n}$ ScMult and $\frac{c_0}{c_n} (c_i k_w k_h - 1)$ Add operations. This method also outputs $\frac{c_0}{c_n}$ ciphertexts.

Table V shows the comparison of our method with existing methods in computation complexity. It is obvious that our method has better complexity, especially for rotation operations. Our experiments demonstrate that this boost substantially speeds up the homomorphic operation of the linear layer.

TABLE V: Computation complexity of each method for convolution

| Method | #Rotation | #ScMul | #Add |
|------------|---|-------------------------------|-------------------------------------|
| GAZELLE | $\frac{c_0 c_i}{c_n^2} (c_n - 1) + \frac{c_i (k_w k_h - 1)}{c_n}$ | $k_w k_h \frac{c_i c_0}{c_n}$ | $\frac{c_0}{c_n} (c_i k_w k_h - 1)$ |
| Our method | $\frac{c_0}{c_n} (c_n - 1) + \frac{c_i (k_w k_h - 1)}{c_n}$ | $k_w k_h \frac{c_i c_0}{c_n}$ | $\frac{c_0}{c_n} (c_i k_w k_h - 1)$ |

APPENDIX E

PROOF OF THEOREM 4.1

Proof. Similar to SIMC, let $\pi_{\text{Non-1in}}^f$ denote the designed protocol for computing the non-linear layer, and $\mathcal{F}_{\text{Non-1in}}^f$ denote the functionality of our protocol (see **Figure 4**). Also, we use Real to represent the real protocol execution of $\pi_{\text{Non-1in}}^f$ between S_0 and the adversary \mathcal{A} compromising S_1 . We will prove that the view of \mathcal{A} in Real is indistinguishable from the view in the simulated execution Sim. We exploit the standard hybrid argument to prove this, where we define three intermediate hybrids, *i.e.*, Hyb₁, Hyb₂ and Hyb₃, and show the indistinguishability of this hybrids in consecutive executions.

Hyb₁: This hybrid execution is identical to Real except in the authentication phase. To be precise, in the authentication phase, the simulator \mathcal{S} use labels $\text{lab}_{i,j}^{\text{out}}$ (described below) to replace the labels $\text{lab}_{i,j}^{\text{out}}$ used in Real. Please note that in this hybrid the simulator \mathcal{S} can access S_0 ' input $\langle \mathbf{u} \rangle_0$ and α , where $\langle \mathbf{u} \rangle_0 + \langle \mathbf{u} \rangle_1 = \mathbf{u}$. Let $\delta = (\mathbf{u} \parallel \text{sign}(\mathbf{u}))$. Therefore, for $i \in$

$[2\kappa]$, we set $\widehat{\text{lab}}_{i,j}^{\text{out}} = \text{lab}_{i,j}^{\text{out}}$ if $j = \delta[i]$, otherwise, $\widehat{\text{lab}}_{i,1-\delta[i]}^{\text{out}}$ (i.e., the ‘‘other’’ label) is set to a random value chosen from $\{0, 1\}^\lambda$ uniformly, where the first bit of $\widehat{\text{lab}}_{i,1-\delta[i]}^{\text{out}}$ is $1 - \xi_{i,\delta[i]}$. We provide the formal description of Hyb_1 as follows, where the indistinguishability between the view of \mathcal{A} in Real and Hyb_1 is directly derived from the authenticity of the garbled circuit (see Section I-F).

1. \mathcal{S} receives $\langle \mathbf{u} \rangle_1$ from \mathcal{A} as the input of OT_λ^κ .
2. Garbled Circuit Phase:
 - For the boolean circuit booln^f , \mathcal{S} first computes $\text{Garble}(1^\lambda, \text{booln}^f) \rightarrow (\text{GC}, \{\{\widehat{\text{lab}}_{i,j}^{\text{in}}, \{\widehat{\text{lab}}_{i,j}^{\text{out}}\}_{j \in \{0,1\}}\}\}_{i \in [2\kappa]})$ for each $i \in [2\kappa]$, and then for $i \in \{\kappa + 1, \dots, 2\kappa\}$ sends $\{\widehat{\text{lab}}_i^{\text{in}} = \widehat{\text{lab}}_{i,(\mathbf{u})_1[i]}^{\text{in}}\}$ to \mathcal{A} as the output of OT_λ^κ . In addition, \mathcal{S} sends the garbled circuit GC and its garbled inputs $\{\{\widehat{\text{lab}}_i^{\text{in}} = \widehat{\text{lab}}_{i,(\mathbf{u})_0[i]}^{\text{in}}\}_{i \in [\kappa]}\}$ to \mathcal{A} .
3. Authentication Phase 1:
 - \mathcal{S} sets $\delta = (\mathbf{u} \parallel \text{sign}(\mathbf{u}))$.
 - For $i \in [2\kappa]$, \mathcal{S} sets $\widehat{\text{lab}}_{i,j}^{\text{out}} = \text{lab}_{i,\delta[i]}^{\text{out}}$ if $j = \delta[i]$.
 - For $i \in [2\kappa]$, if $j = 1 - \delta[i]$, \mathcal{S} sets $\widehat{\text{lab}}_{i,j}^{\text{out}}$ as a random value chosen from $\{0, 1\}^\lambda$ uniformly, where first bit of $\widehat{\text{lab}}_{i,1-\delta[i]}^{\text{out}}$ is $1 - \xi_{i,\delta[i]}$.
 - \mathcal{S} computes and sends $\{ct_{i,j}, \hat{c}_{i,j}\}_{i \in [\kappa], j \in \{0,1\}}$ to \mathcal{A} using $\widehat{\text{lab}}_{i,j}^{\text{out}}_{i \in [2\kappa], j \in \{0,1\}}$. This process is same as in Real execution using $\text{lab}_{i,j}^{\text{out}}_{i \in [2\kappa], j \in \{0,1\}}$.
4. Local Computation Phase: The execution of this phase is indistinguishable from Real since no information needs to be exchanged between \mathcal{S} and \mathcal{A} .
5. Authentication Phase 2:
 - \mathcal{S} randomly selects a fresh shares of authenticated Beaver’s multiplicative triple (A, B, C) , where $C = A \cdot B$.
 - \mathcal{S} sends $\Gamma = \langle \mathbf{u} \rangle_0 - \langle A \rangle_0$ to \mathcal{A} .

Hyb_2 : We will make four changes to Hyb_1 to obtain Hyb_2 , and argue that Hyb_2 is indistinguishable from Hyb_1 from the adversary’s view. To be precise, let $\text{GCEval}(\text{GC}, \{\widehat{\text{lab}}_i^{\text{in}}\}_{i \in [2\kappa]}) \rightarrow \{(\tilde{\xi}_i \parallel \tilde{\zeta}_i)_{i \in [2\kappa]} = \{\widehat{\text{lab}}_i^{\text{out}}\}_{i \in [2\kappa]}\}$. First, we have $\{\widehat{\text{lab}}_i^{\text{out}} = \text{lab}_{i,\delta[i]}^{\text{out}}\}_{i \in [2\kappa]}$ based on the correctness of garbled circuits. Second, we note that ciphertexts $\{ct_{i,1-\tilde{\xi}_i}, \hat{c}_{i,1-\tilde{\xi}_i+\kappa}\}_{i \in [\kappa]}$ are computed by exploiting the ‘‘other’’ set of output labels picked uniformly in Hyb_1 . Based on this observation, \mathcal{S} actually can directly sample them uniformly at random. Third, in real execution, for every $i \in [\kappa]$ and $j \in \{0, 1\}$, S_0 sends $ct_{i,\xi_{i,j}}$ and $\hat{c}_{i,\xi_{i,j}+\kappa}$ to S_1 , and then S_1 computes c_i , d_i and e_i based on them. To simulate this, \mathcal{S} only needs to uniformly select random values c_i , d_i and e_i which satisfy $\langle \alpha \mathbf{u} \rangle_1 = (-\sum_{i \in [\kappa]} c_i 2^{i-1})$, $\langle \text{sign}(\mathbf{u}) \rangle_1 = (-\sum_{i \in [\kappa]} d_i 2^{i-1})$ and $\langle \alpha \text{sign}(\mathbf{u}) \rangle_1 = (-\sum_{i \in [\kappa]} e_i 2^{i-1})$. Finally, since $\langle \alpha \mathbf{u} \rangle_1$, $\langle \text{sign}(\mathbf{u}) \rangle_1$ and $\langle \alpha \text{sign}(\mathbf{u}) \rangle_1$ are part the outputs of functionality $\mathcal{F}_{\text{Non-1in}}^f$, \mathcal{S} can obtain these as the outputs from $\mathcal{F}_{\text{Non-1in}}^f$. In summary, with the above changes, \mathcal{S} no longer needs an input α of S_0 . We provide the formal description of Hyb_2 as follows.

1. \mathcal{S} receives $\langle \mathbf{u} \rangle_1$ from \mathcal{A} as the input of OT_λ^κ .

2. Garbled Circuit Phase: Same as Hyb_1 .
 3. Authentication Phase 1:
 - \mathcal{S} runs $\text{GCEval}(\text{GC}, \{\widehat{\text{lab}}_i^{\text{in}}\}_{i \in [2\kappa]}) \rightarrow \{(\tilde{\xi}_i \parallel \tilde{\zeta}_i)_{i \in [2\kappa]} = \{\widehat{\text{lab}}_i^{\text{out}}\}_{i \in [2\kappa]}\}$.
 - \mathcal{S} learns $\langle \alpha \mathbf{u} \rangle_1$, $\langle \text{sign}(\mathbf{u}) \rangle_1$ and $\langle \alpha \text{sign}(\mathbf{u}) \rangle_1$ by sending $\langle \mathbf{u} \rangle_1$ to $\mathcal{F}_{\text{Non-1in}}^f$.
 - For $i \in [\kappa]$, \mathcal{S} uniformly selects random values c_i , d_i and $e_i \in \mathbb{F}_p$ which satisfy $\langle \alpha \mathbf{u} \rangle_1 = (-\sum_{i \in [\kappa]} c_i 2^{i-1})$, $\langle \text{sign}(\mathbf{u}) \rangle_1 = (-\sum_{i \in [\kappa]} d_i 2^{i-1})$ and $\langle \alpha \text{sign}(\mathbf{u}) \rangle_1 = (-\sum_{i \in [\kappa]} e_i 2^{i-1})$.
 - For every $i \in [\kappa]$, \mathcal{S} computes $ct_{i,\tilde{\xi}_i} = c_i \oplus \text{Trun}_\kappa(\tilde{\zeta}_i)$ and $\hat{c}_{i,\tilde{\xi}_i+\kappa} = (d_i \parallel e_i) \oplus \text{Trun}_{2\kappa}(\tilde{\zeta}_{i+\kappa})$. For ciphertexts $\{ct_{i,1-\tilde{\xi}_i}, \hat{c}_{i,1-\tilde{\xi}_i+\kappa}\}_{i \in [\kappa]}$, \mathcal{S} samples them uniformly at random.
 - \mathcal{S} sends $\{ct_{i,j}, \hat{c}_{i,j}\}_{i \in [\kappa], j \in \{0,1\}}$ to \mathcal{A} .
 4. Local Computation Phase: The execution of this phase is indistinguishable from Real since no information needs to be exchanged between \mathcal{S} and \mathcal{A} .
 5. Authentication Phase 2:
 - \mathcal{S} randomly selects a fresh shares of authenticated Beaver’s multiplicative triple (A, B, C) , where $C = A \cdot B$.
 - \mathcal{S} sends $\Gamma = \langle \mathbf{u} \rangle_0 - \langle A \rangle_0$ to \mathcal{A} .
- Hyb_3 : This hybrid we remove \mathcal{S} ’s dependence on S_0 ’s input $\langle \mathbf{u} \rangle_0$. The indistinguishability between Hyb_3 and Hyb_2 stems from the security of the garbled circuit. We provide the formal description of Hyb_3 below.
1. \mathcal{S} receives $\langle \mathbf{u} \rangle_1$ from \mathcal{A} as the input of OT_λ^κ .
 2. Garbled Circuit Phase:
 - \mathcal{S} samples $\text{Garble}(1^\lambda, \text{booln}^f) \rightarrow (\tilde{\text{GC}}, \{\widehat{\text{lab}}_i^{\text{in}}\}_{i \in \{\kappa+1, \dots, 2\kappa\}})$ and sends $\{\widehat{\text{lab}}_i\}_{i \in \{\kappa+1, \dots, 2\kappa\}}$ to \mathcal{A} as the output of OT_λ^κ . \mathcal{S} also sends $\tilde{\text{GC}}$ and $\{\widehat{\text{lab}}_i^{\text{in}}\}_{i \in [\kappa]}$ to \mathcal{A} .
 3. Authentication Phase 1:
 4. Local Computation Phase: The execution of this phase is indistinguishable from Real since no information needs to be exchanged between \mathcal{S} and \mathcal{A} .
 5. Authentication Phase 2: Same as Hyb_2 , where \mathcal{S} uses $(\langle \mathbf{u} \rangle_1, \tilde{\text{GC}}$, and $\{\widehat{\text{lab}}_i^{\text{in}}\}_{i \in [2\kappa]})$ to process this phase for \mathcal{A} .
 - \mathcal{S} randomly selects a fresh shares of authenticated Beaver’s multiplicative triple (A, B, C) , where $C = A \cdot B$.
 - \mathcal{S} randomly selects $\hat{\Gamma}$ uniformly from \mathbb{F}_p and send it to \mathcal{A} .

APPENDIX F PROTOCOL OF SECURE INFERENCE

In this section, we describe the details of our secure inference protocol (called π_{inf}). For simplicity, suppose a neural network (NN) consists of alternating linear and nonlinear layers. Let the specifications of the linear layer be $\mathbf{N}_1, \mathbf{N}_2, \dots, \mathbf{N}_m$, and the nonlinear layer be f_1, f_2, \dots, f_{m-1} . Given an input vector \mathbf{t}_0 , one needs to sequentially compute

$\mathbf{u}_i = \mathbf{N}_i \cdot \mathbf{t}_{i-1}$, $\mathbf{t}_i = f_i(\mathbf{u}_i)$, where $i \in [m-1]$. As a result, we have $\mathbf{u}_m = \mathbf{N}_m \cdot \mathbf{t}_{m-1} = \text{NN}(\mathbf{t}_0)$. In secure inference, the server S_0 's input is weights of all linear layer, *i.e.*, $\mathbf{N}_1, \dots, \mathbf{N}_m$ while the input of S_1 is \mathbf{t} . The goal of π_{inf} is to learn $\text{NN}(\mathbf{t}_0)$ for the client S_1 . We provide the overview of π_{inf} below and give the details of protocol in **Figure 13**.

Our protocol can be roughly divided into two phases: the evaluation phase and the consistency check phase. We perform the computation of alternating linear and nonlinear layers with appropriate parameters in the evaluation phase. After that, the server performs a consistency check phase to verify the consistency of the calculations so far. The output will be released to client if the check passes.

- **Linear Layer Evaluation:** To evaluate the first linear layer, S_0 and S_1 execute the function **InitLin** to learn $(\langle \mathbf{u}_1 \rangle_b, \langle \mathbf{r}_1 \rangle_b)$ for $b \in \{0, 1\}$, where S_0 's inputs for **InitLin** are (\mathbf{N}_1, α) while S_1 's input is \mathbf{t}_0 . This process is to compute the authenticated shares of \mathbf{u}_1 , *i.e.*, shares of \mathbf{u}_1 and \mathbf{r}_1 . We use \mathbf{r}_1 to represent the authentication of \mathbf{u}_1 . To evaluate the i -th linear layer ($i > 1$), S_0 and S_1 execute the function **Lin** to learn $(\langle \mathbf{u}_i \rangle_b, \langle \mathbf{r}_i \rangle_b, \langle \mathbf{z}_i \rangle_b)$ for $b \in \{0, 1\}$, where S_0 's inputs for **Lin** are $(\langle \mathbf{t}_{i-1} \rangle_0, \langle \mathbf{d}_{i-1} \rangle_0, \mathbf{N}_i, \alpha)$ while S_1 's inputs are $(\langle \mathbf{t}_{i-1} \rangle_1, \langle \mathbf{d}_{i-1} \rangle_1)$. We use \mathbf{d}_{i-1} to denote the authentication on \mathbf{t}_{i-1} . Therefore, **Lin** outputs shares of $\mathbf{u}_i = \mathbf{N}_i \mathbf{t}_{i-1}$, $\mathbf{r}_i = \mathbf{N}_i \mathbf{d}_{i-1}$ and an additional tag $\mathbf{z}_i = (\alpha^3 \mathbf{t}_i - \alpha^2 \mathbf{d}_{i-1})$.
- **Non-Linear Layer Evaluation:** To evaluate the i -th ($i \in [m-1]$) non-linear layer, S_0 and S_1 execute the function $\pi_{\text{Non-1in}}^{f_i}$ to learn $(\langle \mathbf{k}_i \rangle_b, \langle \mathbf{t}_i \rangle_b, \langle \mathbf{d}_i \rangle_b)$ for $b \in \{0, 1\}$, where S_0 's inputs for $\pi_{\text{Non-1in}}^{f_i}$ are $(\langle \mathbf{u}_i \rangle_0, \alpha)$ while S_1 's input is $\langle \mathbf{u}_i \rangle_1$, where we use \mathbf{k}_i to represent another set of shares of authentication on \mathbf{u}_i .
- **Consistency Check Phase:** The server performs the following process to check the correctness of the calculation.
 - For each $i \in \{2, \dots, m\}$, verify that the authentication share entered into the function **Lin** is valid by verifying that $\mathbf{z}_i = 0^{n_i-1}$.
 - For each $i \in [m-1]$, check that the shares input of the function $\pi_{\text{Non-1in}}^f$ is same as the output of **Lin** under the i -th linear layer by verifying that $\mathbf{r}_i - \mathbf{k}_i = 0^{n_i}$.

Finally, all of the above checks can be combined into a single check by S_0 to pick up random scalars. If the check passes, the final prediction can be reconstructed by S_1 , otherwise, S_0 aborts and returns the final share to S_1 .

Correctness. We briefly describe the correctness of our secure inference protocol π_{inf} . In more detail, we first have $\mathbf{u}_1 = \mathbf{N}_1 \cdot \mathbf{t}_0$ and $\mathbf{r}_1 = \alpha \mathbf{u}_1$ by the correctness of **InitLin**.

Then, for each $i \in \{2, \dots, m\}$, we have $\mathbf{u}_i = \mathbf{N}_i \cdot \mathbf{t}_{i-1}$, $\mathbf{r}_i = \mathbf{N}_i \cdot \mathbf{d}_{i-1}$, and $\mathbf{z}_i = \alpha^3 \mathbf{t}_{i-1} - \alpha^2 \mathbf{d}_{i-1}$ by the correctness of **Lin**. Furthermore, for each $i \in [m-1]$, it holds that $\mathbf{k}_i = \alpha \mathbf{u}_i$, $\mathbf{t}_i = f_i(\mathbf{u}_i)$, and $\mathbf{d}_i = \alpha f_i(\mathbf{u}_i)$ by the correctness of $\pi_{\text{Non-1in}}^f$. On the other hand, we can observe that $q = 0$ since for each $i \in [m-1]$, $\mathbf{z}_{i+1} = 0$ and $\mathbf{r}_i = \mathbf{k}_i$. Finally, we have $\mathbf{u}_m = \text{NN}(\mathbf{t}_0)$.

Security. Our secure inference protocol has the same security properties as SIMC, *i.e.*, it is secure against the malicious client model. We provide the following theorem.

Theorem 2. *Our secure inference protocol π_{inf} is secure against a semi-honest server S_0 and any malicious adversary \mathcal{A} corrupting the client S_1 .*

Proof. We leverage simulation-based security to prove that our protocol is secure against the semi-honest server S_0 and the malicious client S_1 . It is easy to demonstrate the security of our protocol for S_0 . Specifically, during the evaluation process of the protocol, S_0 can only learn the shares disclosed during the evaluation. The simulator can choose random values evenly from the field to simulate these shares. Similarly, in the consistency check phase, S_0 learns $\langle q \rangle_1$, which can also be easily simulated by the simulator using $q = 0$, and $\langle q \rangle_0$ can be calculated locally.

We now demonstrate the security of the proposed protocol against malicious clients. Review the ability of a malicious client, *i.e.*, it can arbitrarily violate the configuration of the protocol, especially, send inconsistent input during the execution of the protocol. To be precise, adversary \mathcal{A} can do the following actions: (1) Invoke **InitLin** with input $\mathbf{t}'_0 \neq \mathbf{t}_0$ (client's original input), and learns $\langle \mathbf{u}_1 \rangle_1$ and $\langle \mathbf{r}_1 \rangle_1$; (2) For each $j \in [m-1]$, \mathcal{A} can invoke $\pi_{\text{Non-1in}}^{f_j}$ with input $\langle \mathbf{u}'_j \rangle_1 + \Delta_j^1$, and learn $\langle \mathbf{k}_j \rangle_1$, $\langle \mathbf{t}_j \rangle_1$ and $\langle \mathbf{d}_j \rangle_1$; (3) For each $j \in [m-1]$, \mathcal{A} can invoke **Lin** with inputs $\langle \mathbf{t}'_j \rangle_1 = \langle \mathbf{t}_j \rangle_1 + \Delta_j^2$ and $\langle \mathbf{d}'_j \rangle_1 = \langle \mathbf{d}_j \rangle_1 + \Delta_j^3$, and learn $\langle \mathbf{u}_j \rangle_1$, $\langle \mathbf{t}_j \rangle_1$, and $\langle \mathbf{z}_j \rangle_1$; (4) \mathcal{A} can send an incorrect share of q to S_0 by adding an error Δ^4 to his share. Using the above notation, \mathcal{A} is considered to be honestly following the configuration of the protocol if all Δ 's are 0. We provide a formal simulation of the view of adversary in **Figure 14**.

Based on this, we analyze the following two cases: In the first case, \mathcal{A} did not violate the protocol. It is easy to deduce that the simulated view is exactly the same as the real view. When \mathcal{A} violates the execution of the protocol, we prove that there is a non-zero Δ , so that \mathcal{S} returns abort to the adversary \mathcal{A} with a probability of 1. This is mainly due to the attributes of authentication shares, which guarantees the immutability of data under authentication sharing. Readers can refer to SIMC [10] for more details, which gives a detailed analysis probabilistically. \square

Preamble: Consider a neural network (NN) consists of m linear layers and $m - 1$ nonlinear layers. Let the specifications of the linear layer be $\mathbf{N}_1, \mathbf{N}_2, \dots, \mathbf{N}_m$, and the nonlinear layer be f_1, f_2, \dots, f_{m-1} .

Input: S_0 holds $\{\mathbf{N}_j \in \mathbb{F}_p^{n_j \times n_{j-1}}\}_{j \in [m]}$, i.e., weights for the m linear layers. S_1 holds $\mathbf{t}_0 \in \mathbb{F}_p^{n_0}$ as the input of NN.

Output: S_1 obtains $\text{NN}(\mathbf{t}_0)$.

Protocol:

1. S_0 uniformly selects a random MAC key α from \mathbb{F}_p to be used throughout the protocol execution.
2. **First Linear Layer:** S_0 and S_1 execute the function **InitLin** to learn $(\langle \mathbf{u}_1 \rangle_b, \langle \mathbf{r}_1 \rangle_b)$ for $b \in \{0, 1\}$, where S_0 's inputs for **InitLin** are (\mathbf{N}_1, α) while S_1 's input is \mathbf{t}_0 .
3. For each $j \in [m - 1]$,
 - Non-Linear Layer f_j :** S_0 and S_1 execute the function $\pi_{\text{Non-1in}}^{f_j}$ to learn $(\langle \mathbf{k}_j \rangle_b, \langle \mathbf{t}_j \rangle_b, \langle \mathbf{d}_j \rangle_b)$ for $b \in \{0, 1\}$, where S_0 's inputs for $\pi_{\text{Non-1in}}^{f_j}$ are $(\langle \mathbf{u}_j \rangle_0, \alpha)$ while S_1 's input is $\langle \mathbf{u}_j \rangle_1$.
 - Linear layer $j + 1$:** S_0 and S_1 execute the function **Lin** to learn $(\langle \mathbf{u}_{j+1} \rangle_b, \langle \mathbf{r}_{j+1} \rangle_b, \langle \mathbf{z}_{j+1} \rangle_b)$ for $b \in \{0, 1\}$, where S_0 's inputs for **Lin** are $(\langle \mathbf{t}_j \rangle_0, \langle \mathbf{d}_j \rangle_0, \mathbf{N}_{j+1}, \alpha)$ while S_1 's inputs are $(\langle \mathbf{t}_j \rangle_1, \langle \mathbf{d}_j \rangle_1)$.
4. **Consistency Check:**
 - For $j \in [m - 1]$, S_0 selects $\mathbf{s}_j \in_R \mathbb{F}_p^{n_j}$ and $\mathbf{s}'_j \in_R \mathbb{F}_p^{n_{j+1}}$. S_0 sends $(\mathbf{s}_j, \mathbf{s}'_j)$ to S_1 .
 - S_1 computes $\langle \mathbf{q} \rangle_1 = \sum_{j \in [m-1]} ((\langle \mathbf{r}_j \rangle_1 - \langle \mathbf{k}_j \rangle_1) \cdot \mathbf{s}_j + \langle \mathbf{z}_{j+1} \rangle_1 \cdot \mathbf{s}'_j)$ and sends it to S_0 .
 - S_0 computes $\langle \mathbf{q} \rangle_0 = \sum_{j \in [m-1]} ((\langle \mathbf{r}_j \rangle_0 - \langle \mathbf{k}_j \rangle_0) \cdot \mathbf{s}_j + \langle \mathbf{z}_{j+1} \rangle_0 \cdot \mathbf{s}'_j)$.
 - S_0 aborts if $\langle \mathbf{q} \rangle_0 + \langle \mathbf{q} \rangle_1 \pmod p \neq 0$. Else, sends $\langle \mathbf{u}_m \rangle_0$ to S_1 .
5. **Output Phase:** S_1 outputs $\langle \mathbf{u}_m \rangle_0 + \langle \mathbf{u}_m \rangle_1 \pmod p$ if S_0 didn't abort in the previous step.

Figure 13: Secure inference protocol π_{inf}

Preamble: \mathcal{S} interacts with an adversary \mathcal{A} that controls S_1 , where the input of S_1 is \mathbf{t}_0 . \mathcal{S} sets a flag bit $\mathbf{flag} = 0$.

- **First Linear Layer:** \mathcal{S} execute the function **InitLin** with input \mathbf{t}'_0 , and then sends $\langle \mathbf{u}_1 \rangle_1$ and $\langle \mathbf{r}_1 \rangle_1$ to \mathcal{A} .
- For each $j \in [m - 1]$,
 - Non-Linear Layer f_j :** \mathcal{S} execute the function $\pi_{\text{Non-1in}}^{f_j}$ with input $\langle \mathbf{u}'_1 \rangle_1 + \Delta_j^1$, and then sends uniform $\langle \mathbf{k}_j \rangle_1, \langle \mathbf{t}_j \rangle_1$ and $\langle \mathbf{d}_j \rangle_1$ to \mathcal{A} . \mathcal{S} sets a flag bit $\mathbf{flag} = 1$ if $\Delta_j^1 \neq 0^{n_j}$.
 - Linear layer $j + 1$:** \mathcal{S} execute the function **Lin** with inputs $\langle \mathbf{t}'_j \rangle_1 = \langle \mathbf{t}_j \rangle_1 + \Delta_j^2$ and $\langle \mathbf{d}'_j \rangle_1 = \langle \mathbf{d}_j \rangle_1 + \Delta_j^3$, and then sends uniform $\langle \mathbf{u}_j \rangle_1, \langle \mathbf{t}_j \rangle_1$, and $\langle \mathbf{z}_j \rangle_1$ to \mathcal{A} . In addition, \mathcal{S} sets a flag bit $\mathbf{flag} = 1$ if $(\Delta_j^2, \Delta_j^3) \neq (0^{n_j}, 0^{n_j})$.
- 4. **Consistency Check:**
 - For $j \in [m - 1]$, \mathcal{S} selects $\mathbf{s}_j \in_R \mathbb{F}_p^{n_j}$ and $\mathbf{s}'_j \in_R \mathbb{F}_p^{n_{j+1}}$. \mathcal{S} sends $(\mathbf{s}_j, \mathbf{s}'_j)$ to S_1 .
 - \mathcal{A} computes $\langle \mathbf{q} \rangle_1 = \Delta^4 + \sum_{j \in [m-1]} ((\langle \mathbf{r}_j \rangle_1 - \langle \mathbf{k}_j \rangle_1) \cdot \mathbf{s}_j + \langle \mathbf{z}_{j+1} \rangle_1 \cdot \mathbf{s}'_j)$ and sends it to \mathcal{S} . \mathcal{S} set $\mathbf{flag} = 1$ if $\Delta^4 \neq 0$.
- 5. **Output Phase:** \mathcal{S} obtains $\text{NN}(\mathbf{t}'_0)$ and send $\text{NN}(\mathbf{t}'_0) - \langle \mathbf{u}_m \rangle_1$ to \mathcal{A} if $\mathbf{flag} = 0$. Otherwise, it sends abort to both π_{inf} and \mathcal{A} .

Figure 14: Simulator against malicious client for π_{inf}